Alfred-Wegener-Institut
für Polar und Meeresforschung
in der Helmholtz-Gemeinschaft

JACOBS UNIVERSITY

The Laptev Sea inshore zone modeling with focus on the Lena Delta region

Ph.D. Thesis Proposal

Vera Fofonova

October 2012

Helmholtz Graduate School for Polar and Marine Research
Jacobs University Bremen
Alfred-Wegener-Institute for Polar and Marine Research

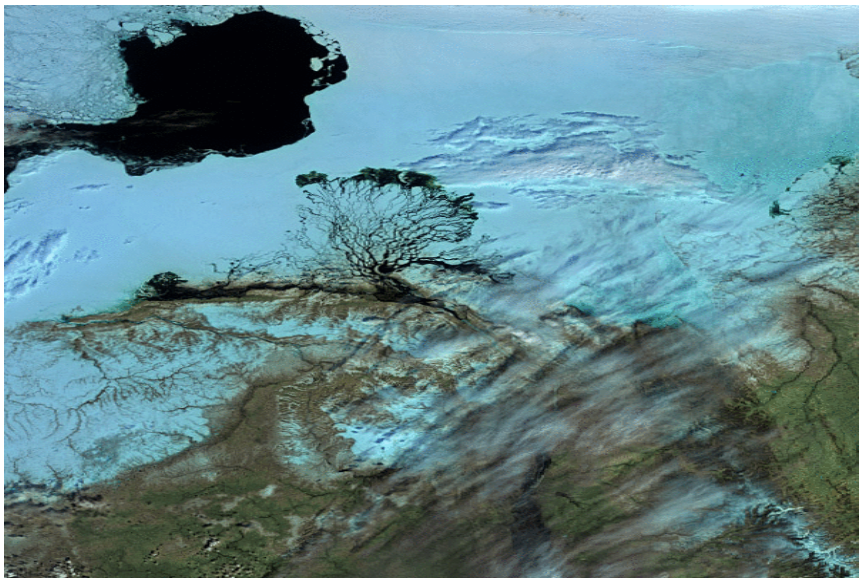

Dissertation Committee

Prof. Dr. Karen Helen Wiltshire

Professor of Marine Geosciences

Jacobs University Bremen

Biosciences – Shelf Sea Ecology

Alfred-Wegener-Institute Helgoland

Dr. Sergey Danilov

Climate Sciences - Climate Dynamics

Alfred-Wegener-Institute Bremerhaven

Prof. Dr. Vikram Unnithan

Professor of Geosciences

School of Engineering & Science

Jacobs University Bremen

Dr. Jens Schröter

Climate Sciences - Climate Dynamics

Alfred-Wegener-Institute Bremerhaven

Contents

Introduction

The polar shelf zones are highly dynamic and diverse systems. They form a border between warm and fresh water continental drain and the salty currents of the northern seas. In the Arctic shelf region multiple river deltas accumulate organic carbon. They host a unique and very diverse northern fauna and flora. The Lena River discharge ranks 8th in the world. Its average annual runoff into the Laptev Sea is 541km^3 (RosHydromet, web source). The Lena delta region of the Laptev Sea can serve as an indicator of climate change. A large number of observations in this region suggest a strong climate and biological data changes for the last fifty years. As part of International Polar Year (2007 - 2008 years) scientists from The National Research Center of France, University of Alaska (USA), Melnikov Permafrost Institute (Siberian Branch of Russian Academy of Sciences) organized an expedition for impact assessment the climate changes to Lena River dynamics. It was found that the Lena water temperature in the flood period had increased by 2 ° C compared to the values of 1950 (Costard et al., 2007).

Based on the results of observations in the Lena Delta region (Russian-German expeditions «Lena-2007», «Lena-2008») and Laptev Sea (Russian-German expedition «BARKALAV-2007/TRANSDRIFT-XII», «POLYNIA-2008/TRANSDRIFT-XIII», «BARKALAV-2008/TRANSDRIFT-XIV») it was established, that in summer 2007 a positive anomaly of temperature and negative of salinity existed in the central and eastern part of the Laptev Sea in the mixed layer. The same structure of temperature and salinity field was observed in summer 2008, but the magnitudes of anomalies were smaller. A continuant temperature increase was also found for Atlantic water. Such a powerful invasion of warm Atlantic waters into the Arctic Basin was not previously observed for the entire period of instrumental observations since 1897 (AARI, web source).

Structure of pelagic communities and food webs on the shelf of the Laptev Sea directly depends on the fresh water plume dynamics and temperature variations and varies from year to year. At this stage it is particularly important to estimate the role of different factors to dynamics in the region.

One of the main questions for biologists also is as to how the shifts of chemical water composition will affect the sea shelf aquatic community diversity and functioning and the coastal productivity. Several fundamental questions arise: (i) should we expect major shifts in the seasonal hydrography patterns and related changes in biological productivity; (ii) to which degree the change in coastal flows will influence the transport routes of marine organisms and chemical compositions?

One of the goals of my PhD is to evaluate dynamics of the hydrography-carbon transport in Lena Delta region of the Laptev Sea, in recent decades. In framework of this

purpose **the first task** is to tune a basic numerical model which is able to reproduce the climatic changes in the region. The model should provide adequate information about salinity, temperature, water elevation, sea - ice fraction and ice flow and dynamics of fresh water distribution in the Lena Delta region of the Laptev Sea in the presence of high-quality initial data. The special attention should be paid to tidal dynamics according to fast ice mask. The Arctic tides are sensitive to the presence of ice cover and the availability of inertial current shear to drive mixed in the Arctic shelf seas depends of sea-ice conditions.

The second task is to assess the variability of the climate system, i.e. to analyze the role of individual factors in observed changes.

The third task is to implement a biological module in to the Laptev Sea shelf 3D model. This module would act as a platform that would allow users to examine the relative importance of different physical and biological processes under well-calibrated physical fields.

Background

General description of the Laptev Sea region

The Laptev Sea lies to the east of the Taymyr Peninsula and Severnaya Zemlya, extending to the Novosibirsk Islands. The Laptev and East Siberian Seas have the most severe climate and the lowest salinity of all the seas of the northern coast of Asia (Zenkevitch, 1963). Among the seas of the Arctic Ocean into the Laptev Sea the largest number of rivers flows: Lena (provides approximately 70% of total runoff to the Laptev Sea), Olenyok, Khatanga, Anabar, Yana, Omoloy, Gusiha and other small. The total amount of annual flow into the Laptev Sea is more than 700 km^3 . The Laptev Sea shores are winding and form gulfs and bays of various sizes, the coastal landscape is also diverse (Dobrovolsky, Zalogin, 1982).

The main gulfs of the Laptev Sea coast are the Khatanga Gulf, the Olenyok Gulf, the Buor-Khaya Gulf and the Yana Bay. There are several dozens of islands with the total area of 3,784 km^2, mostly in the western part of the Laptev Sea and in the river deltas. The area of the Laptev Sea is 650,000 km^2; its volume is 338,000 km^3 (web source, Great Soviet Encyclopedia).

As in the Kara Sea, a deep gully enters the western part of the Laptev Sea from the north; saline and somewhat warmer waters flow into the Laptev Sea through it. To the east of the northern end of Taymyr the great depths of the Arctic basin approach nearest to the Asian coast, lying only 100 to 200 km off the Severnaya Zemlya and Taymyr shores. The average depth of the Laptev Sea is 519 m and its greatest depth is 2,980 m. However, the dominant depth is about 50-100m (Fig. 1).

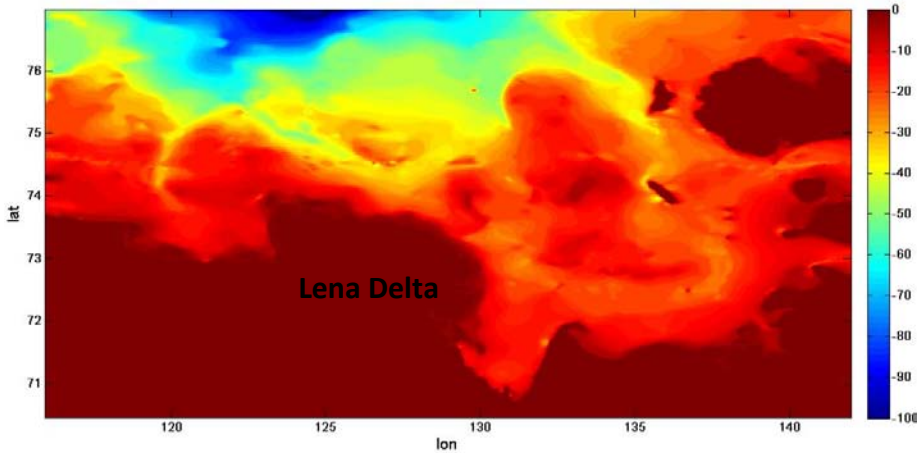

Fig. 1. The seabed topography based on GEBCO bathymetry data, m (0m – terrestrial area).

The bottom of the southern Laptev Sea presents quite a sloping plain, lowering to the north, cut by canyon-like troughs, which are now only weakly pronounced. These troughs are all located at the mouths of rivers, entering the sea from the south. The underwater troughs appear to be the traces of the river valleys which crossed the low plain many millennia ago (Kotyukh et al., 1990).

From the point of view of the problem the bathymetry map of Lena Delta region of the Laptev Sea is of particular interest. The observation bathymetry data at 27686 locations (the average distance between points is about 800m) in close proximity to Lena Delta were provided by Paul Overduin (Alfred Wegener Institute, Potsdam). The Lena Delta zone bathymetry map based on observation data is shown on the Fig. 2.

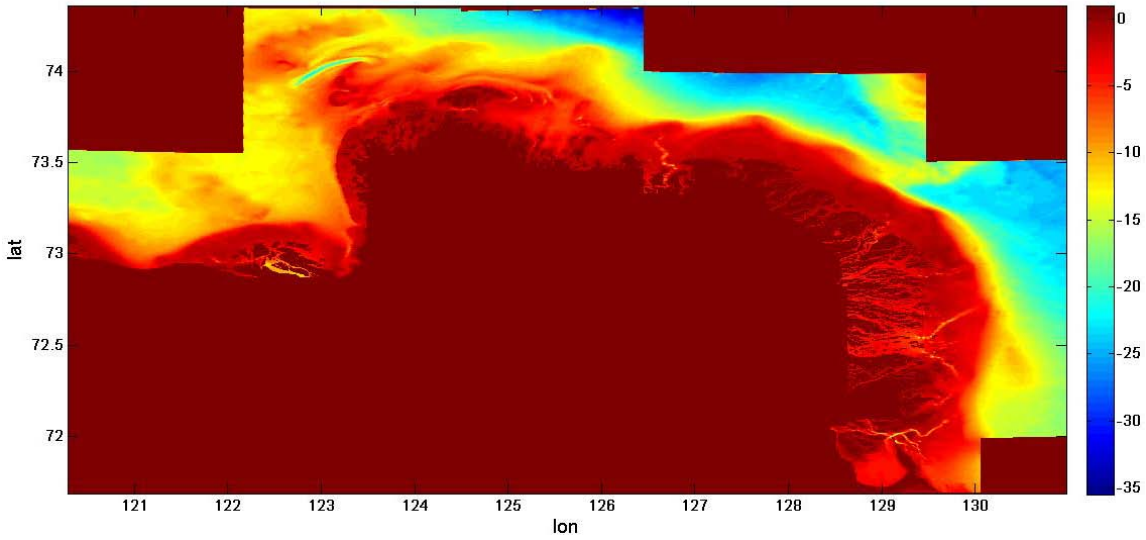

Fig. 2. The seabed topography based on bathymetry data of AWI (Potsdam), m (0m – terrestrial area).

The Laptev Sea is jokingly referred to as the cemetery of cyclones by synopticians (Timokhov, 1994). Wind speed over the sea is an average 5 m/s, storms occur in the Laptev Sea three to four times monthly. Cloudiness remains slight and precipitation is also less than in other regions. Solar radiation, continuously impacting the region during the entire polar day, plays the main role in its impact on climate. In summer, atmospheric circulation is weaker. Relative humidity reaches 95-98 %, which is why fog is quite frequent, especially in regions with considerable ice accumulation (Timokhov, 1994).

Temperature and salinity patterns

The long-term analysis by (Polyakov et al., 2008) of the surface salinity change in the Arctic Basin and Arctic Seas, including the Laptev Sea, showed, that ice-related processes, freshwater runoff and its spreading under the influence of atmospheric processes play a key role in desalination and salinity changes of the upper layer over the past decades.

The atmospheric forcing greatly determines the direction of freshwater transport in the Laptev Sea as was shown by modeling studies (Johnson, 2001). The observations have confirmed that the variability of summer surface salinity in the Laptev Sea is mainly governed by local wind patterns associated with positive and negative phases of atmospheric vorticity over the adjacent Arctic Ocean (Dmitrenko et al., 2005). It should be emphasized that the winter water dynamics has very small impact to riverine water pathways in the summer (Dmitrenko et al., 2010a). The shelf waters below the pycnocline in the southern Laptev Sea inner shelf conserve for at least one seasonal cycle from summer to late winter/spring season the following year (Bauch et al., 2009), (Dmitrenko et al., 2010a). In the end of the winter season (March-April) the surface hydrography pattern is nearly the same as in September modified by thermodynamic ice formation. The thermodynamic ice formation and small Lena river freshwater impact provide in the end of winter season surface salinity increase of ~5 PSU (Dmitrenko et al., 2010a) (Fig.3).

The warm intermediate layer in Laptev Sea is mostly observed during all seasons and its features are first order independent from inter-annual variations.

The prevailing cyclonic regime (positive vorticity) in the summer leads to spread of the Laptev Sea riverine water to the east and hence a negative salinity anomaly east of the Lena Delta and farther to the East Siberian Sea, and a positive anomaly to the north of the Lena Delta. The prevailing of anticyclonic regime (negative vorticity) in the summer leads negative salinity anomalies northward from the Lena Delta due to freshwater advection toward the north, and a corresponding salinity increase eastward (Dmitrenko et al., 2005).

The ocean surface anticyclonic circulation regime in the Arctic saved between 1997 and 2011, only in 2009 the annual wind-driven ocean circulation regime can be characterized as short-lived cyclonic. The anticyclonic regime has dominated for at least 14 years instead of the typical 5-8 year duration (Proshutinsky et al., 2011). The seasonal climatological cycle in the Arctic is characterized by the dominance of anticyclonic ice and ocean circulation in winter and cyclonic circulation in summer. Despite the fact that the anomalies of atmospheric circulation play significant role on

local salinity and temperature patterns, surface salinity field over the shelf area east of the Lena Delta is an invariant to atmospheric circulation, standard deviation is varying between 2 and 4 PSU (Dmitrenko et al., 2010a) (Fig. 3). Apparently, an as of yet undetermined interplay between atmospheric circulation, river runoff, topography and ice related processes may explain those components of the salinity variance that are not well described by local wind patterns (Dmitrenko et al., 2005).

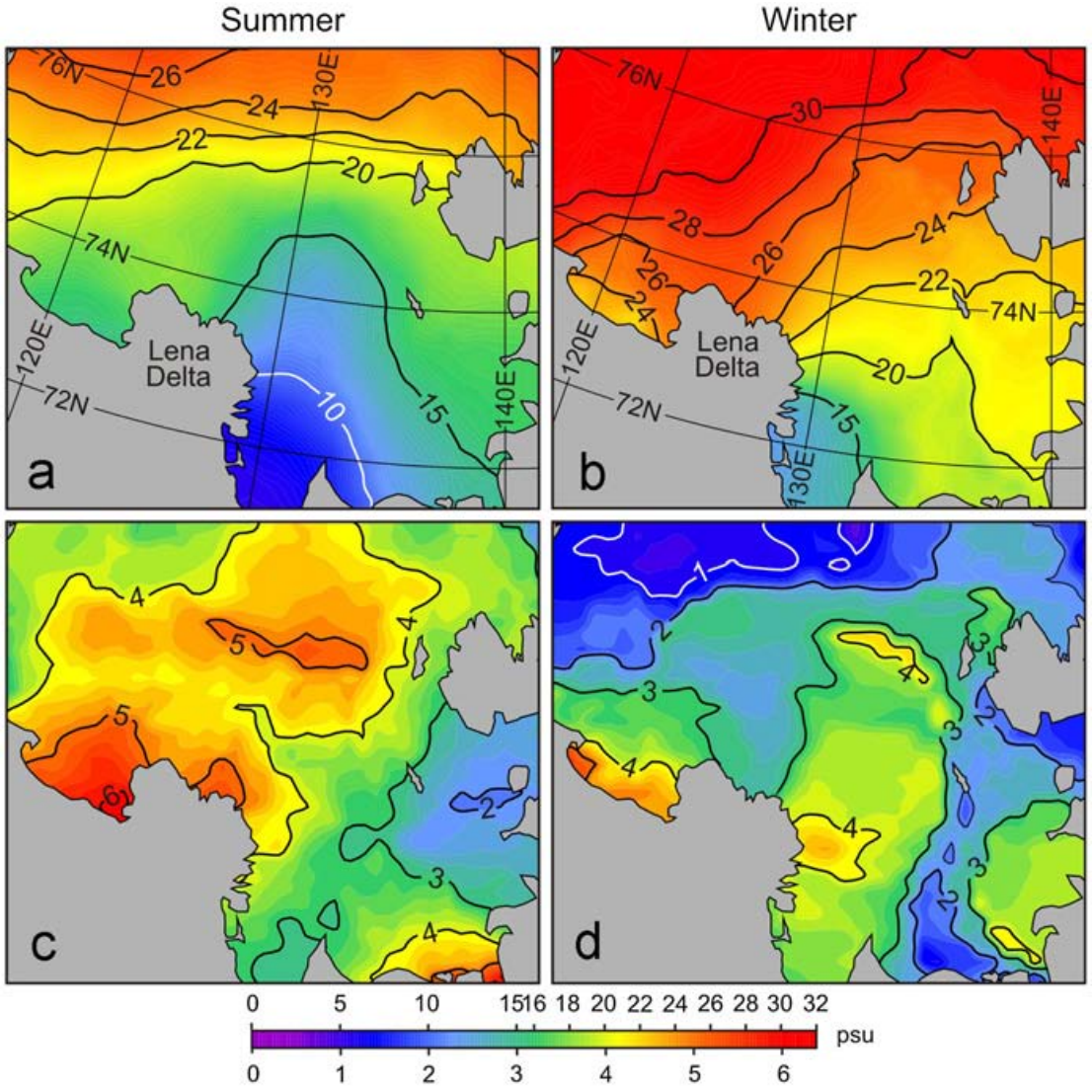

Fig. 3. Long-term mean (1920–2008) surface salinity distribution, PSU for a) summer (July–September) and b) winter (February–April), with their standard deviations in panels c) and d), respectively. The picture is taken from (Dmitrenko et al., 2010a).

The climatology of bottom hydrography demonstrates warming that extends offshore from the 30–50 m depth contour (Fig. 4). Based on historical records of bottom layer temperature was found that the Laptev Sea outer shelf links to the Arctic Ocean Atlantic water boundary current transporting warm and saline water from the North Atlantic (Dmitrenko et al., 2010b). The intrusions are typically about 0.2°C warmer and 1–1.5

practical salinity units saltier than ambient water. The Atlantic water warming of the mid-1990s and the mid-2000s is consistent with outer shelf bottom temperature variability. But there is no significant warming over the Laptev Sea shelf deeper than 10–15 m in the historical record (Dmitrenko et al., 2010b).

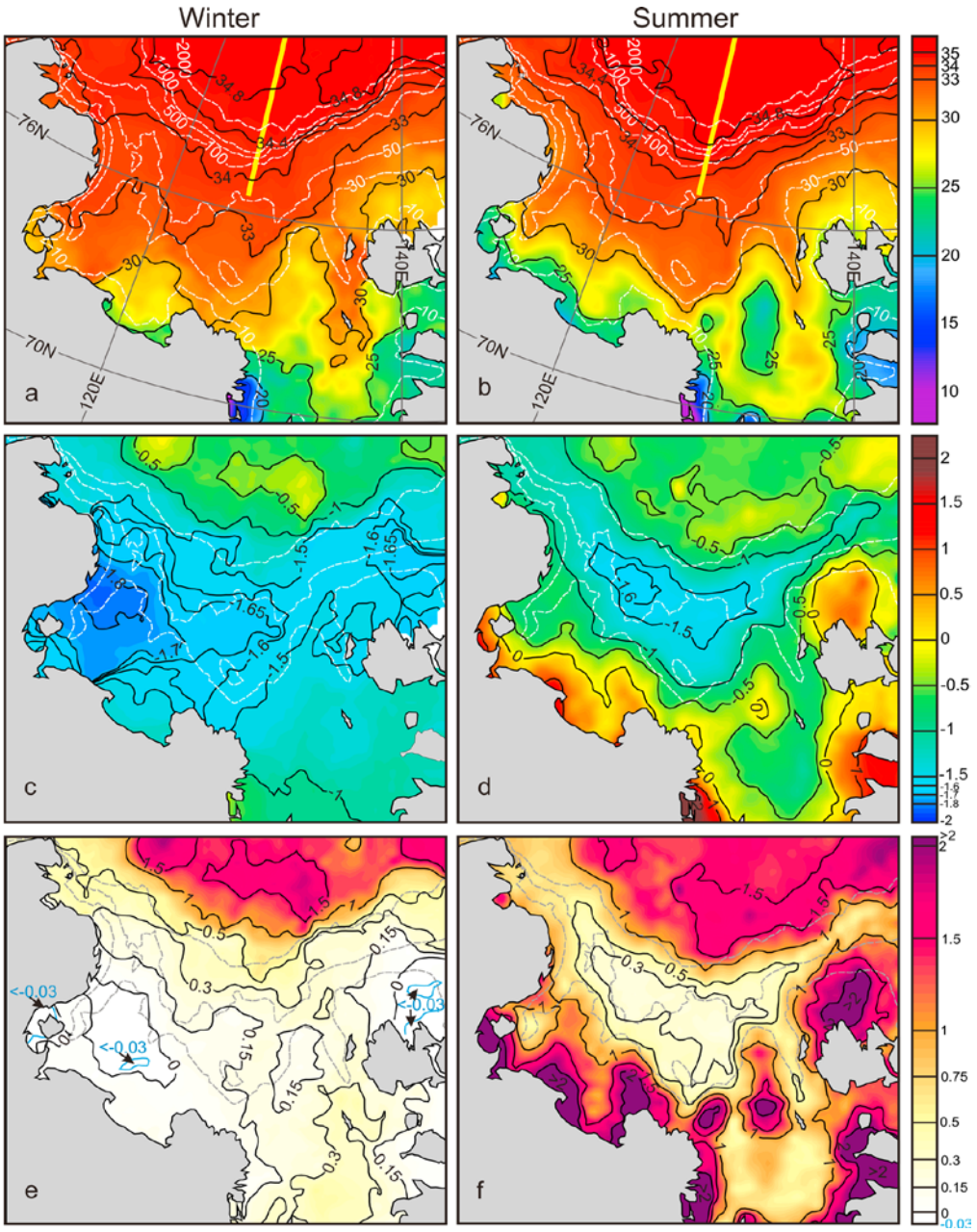

Fig. 4. The long-term mean (1930s-2000s) bottom salinity (a,b), PSU, temperature (c,d), °C, and (e,f) difference between the observed and the freezing temperature, °C, for winter (left) and summer (right). Dashed lines show the 10, 30, 50, 100, 500, 1000 and 2000 m depth contours. Yellow line on the top indicates CTD cross-slope transect occupied annually in August-October from 2002 to 2009. The picture is taken from (Dmitrenko et al., 2010b).

Ice conditions

Among the Siberian shelf seas the Laptev Sea is considered one of the most significant regions of net ice production and export (Zakharov, 1966) (Dethleff et al., 1998). With an average outflow of 483,000 km^2 per year over the period 1979–1995, it contributes more sea ice than the Barents Sea, Kara Sea, East Siberian Sea and Chukchi Sea combined (Dobrovolsky, Zalogin, 1982), (Alexandrov et al., 2000). About 20% of the ice transported through Fram Strait is produced in the Laptev Sea (Rigor and Colony, 1997). Thereby the Laptev Sea ice conditions play a key role in the future fate of the Arctic sea ice.

The Laptev Sea is ice covered from October to June (Bareiss and Goergen, 2005). In August and September the Laptev Sea is more often almost free of ice. The ice formation starts in September on the north and October on the south. It results in a large continuous sheet of ice, with the thickness up to 2 meters in the south-eastern part of the Sea as well as near the coast (Alexandrov et al., 2000). The ice cover can be divided into three types: the fast ice, the pack ice, and flaw polynyas (Eicken et al., 2005)(Fig. 5). The coastal sheet (fast ice) ends at the water depth of about 20–25 m, fast ice is observed up to several hundred kilometers from the shore, and it covers approximately 30% of the Sea area. The latent heat polynyas with high ice production are formed north to this fast ice border by the warm south winds around there. They have various names, such as the Great Siberian Polynya, and can stretch over many hundreds kilometers (Dobrovolsky, Zalogin, 1982) (Fig. 5). The polynyas activity varies greatly from year to year. The freely floating ice pack offshore of the fast ice edge consists mainly of ice formed during fall. According to systematic observations carried out by the Soviet Union since the 1930s, it reaches a mean thickness of 1.57m±0.25m (Romanov, 1996). The pack ice drift is dominated by persistent offshore winds leading to a continuous export of ice out of the Laptev Sea into the basin and/or the East Siberian Sea (Timokhov, 1994).

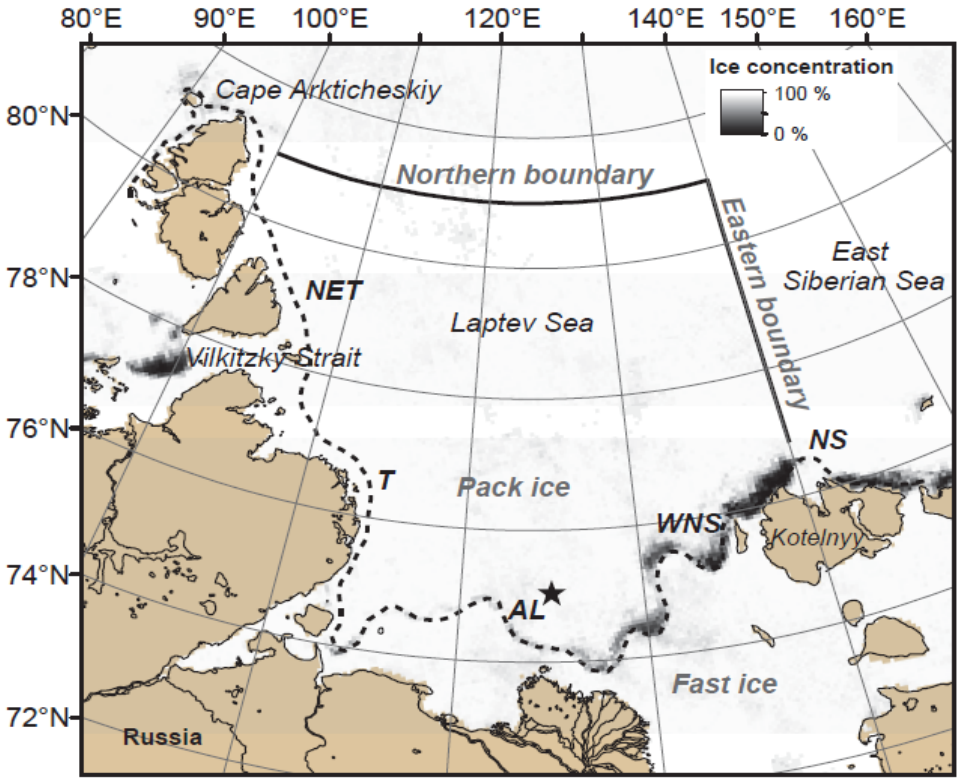

Fig. 5. The geographical location of the Laptev Sea and the northern and eastern boundaries (solid black lines) on which meridional and zonal ice area flux estimates are based. The dashed line represents the mean fast ice edge location. Between pack ice and fast ice edge, flaw polynyas are formed: The New Siberian polynya (NS), the Western New Siberian polynya (WNS), the Anabar-Lena polynya (AL), the Taymyr polynya and the North-Eastern Taymyr (NET) polynya. Color coding corresponds to the sea ice concentration as obtained from Advanced Microwave Scanning Radiometer (AMSR-E) on 7 May 2008. The positions of the moorings used for satellite ice motion data validation are indicated by black stars. The picture is taken from (Krumpen et al., 2012).

In recent years, the summer Arctic sea ice extent and thickness have changed dramatically. The total sea ice extent is declining at an annual rate of approximately 3% per decade over the satellite records (1978–present). The summer sea ice decline seems to be accelerating (Stroeve et al., 2008), (Kwok and Rothrock, 2009), (Comiso, 2010).The rapid reduction in Arctic summer ice extent and thickness is assumed to result from anomalously high surface air temperatures (Stroeve et al., 2008) and changes in the large-scale atmospheric circulation (Meier et al., 2007), (Krumpen et al., 2012). For example, the combined global land and ocean surface temperature in 2007 fell within the 10 highest on record while the average land temperature was the warmest since global records began in 1880. Also the 2007 was named the warmest year for Russia (based on air temperature data) since the late nineteenth century. Almost 40% of the Arctic

sea-ice cover that was present in the 1970s was lost by 2007 during the record low in summer sea-ice extent. (Hölemann et al., 2011).

The seasonal and interannual variability of Laptev Sea ice exchange with the surrounding seas was first examined by Zakharov (1966b, 1967). According to the latest research by Krumpen et al. (2012) it was found:

- The average winter (October to May) ice area transport across the northern and eastern Laptev Sea boundaries (NB and EB) (Fig. 5) is about 3.48×10^{5} km^2.
- The average transport across the NB (2.87×10^{5} km^2) is thereby higher than across the EB (0.61×10^{5} km^2), with a less pronounced seasonal cycle. The total Laptev Sea ice area flux significantly increased over the last decades (0.85×10^{5}km^2/decade, $p > 0.95$), dominated by increasing export through the EB (0.55×10^{5}km^2/decade, $p > 0.90$), while the increase in export across the NB is small (0.3×10^{5} km^2/decade) and statistically not significant.
- The strong coupling between across-boundary SLP gradient and ice drift velocity indicates that monthly variations in ice area flux are primarily controlled by changes in geostrophic wind velocities, although the Laptev Sea ice circulation shows no clear relationship with large-scale atmospheric indices. Also there is no evidence of increasing wind velocities that could explain the overall positive trends in ice export.
- Most of the ice that is incorporated into the Transpolar Drift is formed during freeze-up and originates from the central and western part of the Laptev Sea, while the exchange with the East Siberian Sea is dominated by ice coming from the Central and South-Eastern Laptev Sea.

Following Spreen et al. (2011), they assumed that changes in ice flux rates may be related to changes in the ice cover such as thinning and/or a decrease in concentration. Krumpen et al. (2012) results imply that the late winter (February to May) ice area flux may at least partially control the summer sea ice extent in the Laptev Sea.

Tidal dynamics

The eastern Siberian shelf, consisting of the Laptev and East Siberian Seas, is the shallowest of the entire World Ocean, with an average depth of about 20–30 m (Dmitrenko et al., 2008a). This topographic feature makes the eastern Siberian shelf very sensitive to the tidal mixed processes that dominate the eastern Siberian shelf environments. Both winds and tides contribute to mixed on the Arctic continental shelf seas. Also tides provide direct forcing to the Arctic marginal Seas in all seasons (Lenn et al., 2011). The Arctic tides are sensitive to the presence of ice cover and the availability of inertial current shear to drive mixed in the Arctic shelf seas depends of sea-ice conditions (Kowalik, 1994), (Lenn et al., 2011). Satellite imagery from RADARSAT showed persistent oscillatory ice motion at mixed inertial–tidal frequencies (Kwok et al., 2003). The knowledge of ice–tide interaction still has numerous gaps.

In dissertation work by (Sof'ina, 2008) on the topic 'The simulation of tidal ice drift and ice-related changes in tidal dynamics and energy in Siberian continental shelf' among other results were calculated tidal map, barotropic ellipses and maximal velocity of tidal ice drift for M2 constituent on the assumption that the Siberian continental shelf is covered by movable ice with 2m thickness. The simulations were based on QUODDY-4 (Fig. 6). In this work also was found that the presence of ice leads uneven redistribution of barotropic velocities with both positive and negative additive compared with the result of simulation on the assumption that the Siberian continental shelf is in the ice free.

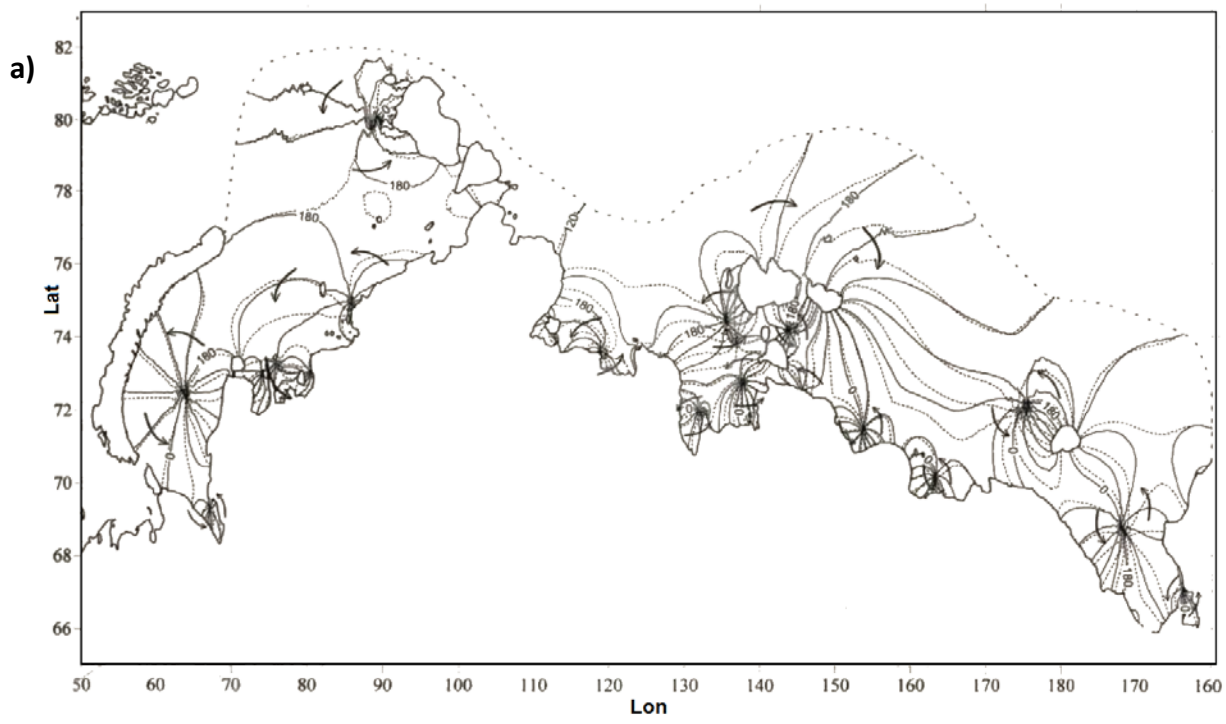

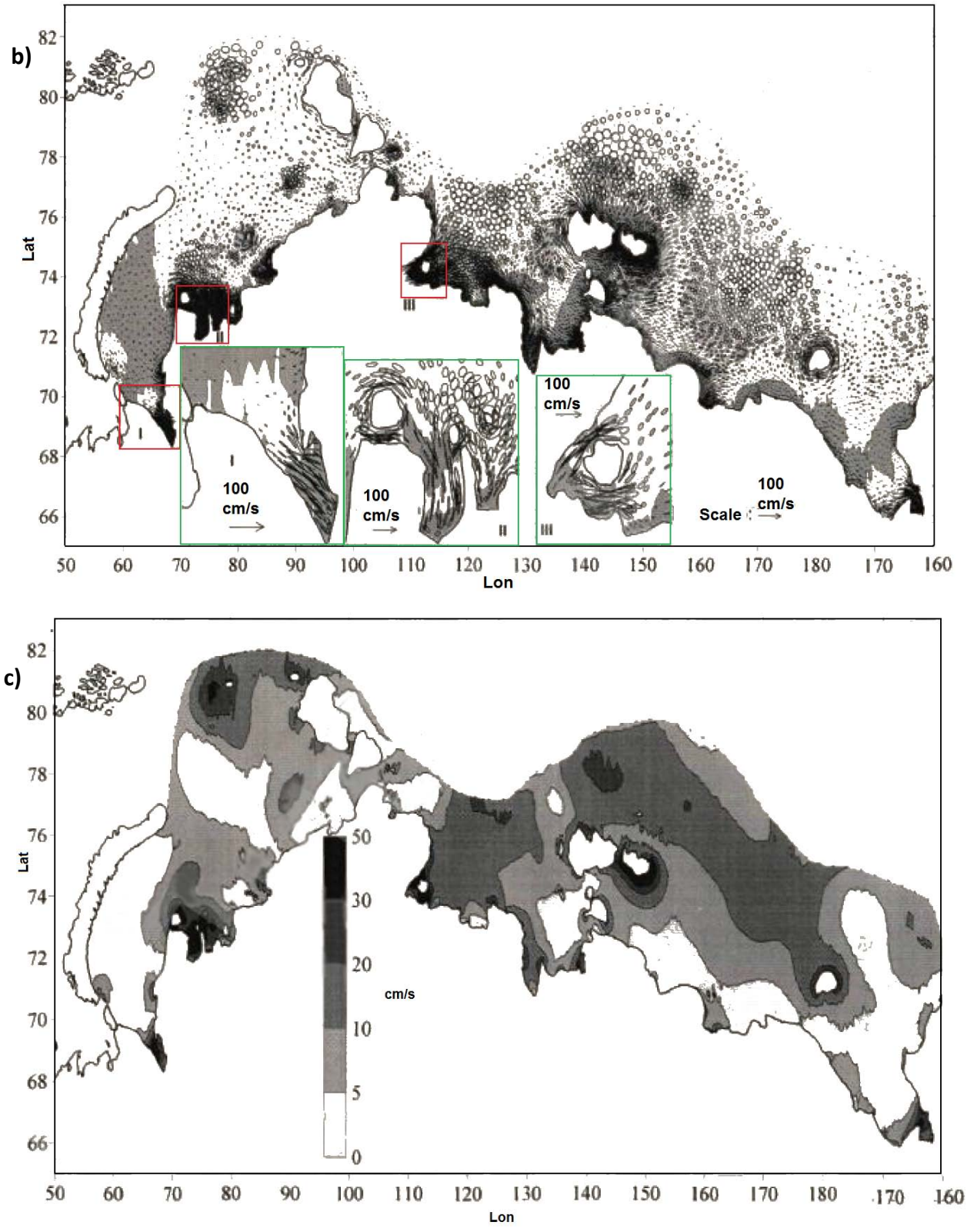

Fig. 6. The results of simulations of M2 constituent dynamics and energetic on the assumption that the Siberian continental shelf is covered by movable ice with 2m thickness: a) Tidal map, b) Ellipses (the ellipses with counterclockwise rotation of the velocity vector are shaded), c)Maximal barotropic velocity of tidal ice drift.

Observations of tidal currents over the Laptev Sea continental slope are rare and fragmentary. Analysis of an approximately 6-month-long ADCP record from 2004–2005,which was made by (Dmitrenko et al., 2008b), showed that the semidiurnal lunar tide (M2, period ~12.42 h) was dominant with a maximal 4–5 cm s^{-1} amplitude of tidal current. Recent studies by (Lenn et al., 2011) confirmed that semidiurnal tides dominate tidal currents at the mooring located over the Laptev Sea slope (76°44' N, 125°55' E). Pnyushkov and Polyakov (2011) harmonic and spectral analyses of currents based on two years-long (2004–05 and 2005–06) records from two moorings deployed at the continental slope of the Laptev Sea (78°26´N, 125°40´E) showed that the semidiurnal tidal constituent S2 dominates over the semidiurnal M2 and diurnal constituents. This dominance of the S2 constituent in the tidal currents is due to resonant interaction of the super inertial wave with sloping bottom topography (Pnyushkov and Polyakov, 2011). However according to tidal model with observation data assimilation by L. Padman and S. Erofeeva sea level changes are dominated by the M2 constituent, in contrast to the tidal currents.

Dmitrenko et al. (2012), based on the CTD and ADCP data obtained in April–May 2008 and April 2009 at two mooring sites located along the land-fast ice edge over the southeastern Laptev Sea shelf data, showed the modification of the shelf halocline layer (SHL) stratification through the appearance of nearly homogeneous water layers. Estimates of the gradient Richardson numbers from the 2008 observations provided evidence that the velocity shear associated with semidiurnal baroclinic tidal flow may be strong enough to play a role in water mass modification, promoting shear instabilities, turbulence, and vertical mixed of seawater properties across the SHL. They also showed a striking feature of the tidal flow: the increased amplitude of the semidiurnal tidal flow velocity at the depth range of the SHL, indicating significant shear in the tidal currents. In 2008, the major axis amplitude for the lunar semidiurnal M2 tidal ellipses demonstrated intermediate maximum in the SHL at 11–13 m (15$\pm$3 cm/s), gradually decreasing to sub ice and near-bottom layers to ~ 9$\pm$3 cm/s (at 7 m) and 7$\pm$2cm/s (at 19 m), respectively. In 2009, the semidiurnal tidal flow exhibited similar patterns, but velocities were reduced by about factor of 2. The tidal analysis by (Dmitrenko et al., 2012) revealed the dominance of the lunar semidiurnal constituent M2 (78$\pm$3% and 72$\pm$15% of the tidal energy in 2008 and 2009, respectively, depending on depths) with a depth-dependent amplitude ranging from 9 to 16 cm/s in 2008 and from 5 to 9 cm/s in 2009. The concurrent solar semidiurnal constituent S2 with a period of half a solar day contributes 21$\pm$3% and 16$\pm$7% in 2008 and 2009, respectively, with a depth-dependent amplitude ranging from 5 to 8 cm/s in 2008, and from 2 to 4 cm/s in 2009. The contribution of the K1 and O1 constituents is negligible.

Model description

To perform designated tasks we are using Finite Volume Coastal Ocean Model (called FVCOM) (Chen et al., 2006). FVCOM was originally developed by UMASSD-WHOI for the estuarine flooding/drying process in estuaries and the tidal-, buoyancy- and wind-driven circulation in the coastal region featuring with complex irregular geometry and steep bottom topography. FVCOM is a prognostic, unstructured-grid, finite-volume, free-surface, 3-D primitive equation coastal ocean circulation model (Chen et al., 2006), (Chen et al., 2003).

The governing equations in Cartesian Coordinates consist of the following momentum, continuity, temperature, salinity, and density equations:

$$\frac{\partial u}{\partial t}+u\frac{\partial u}{\partial x}+v\frac{\partial u}{\partial y}+w\frac{\partial u}{\partial z}-fv=-\frac{1}{\rho_0}\frac{\partial P}{\partial x}+\frac{\partial}{\partial z}\left(K_m\frac{\partial u}{\partial z}\right)+F_u$$

$$\frac{\partial v}{\partial t}+u\frac{\partial v}{\partial x}+v\frac{\partial v}{\partial y}+w\frac{\partial v}{\partial z}+fu=-\frac{1}{\rho_0}\frac{\partial P}{\partial y}+\frac{\partial}{\partial z}\left(K_m\frac{\partial v}{\partial z}\right)+F_v$$

$$\frac{\partial P}{\partial z}=-\rho g$$

$$\frac{\partial u}{\partial x}+\frac{\partial v}{\partial y}+\frac{\partial w}{\partial z}=0$$

$$\frac{\partial T}{\partial t}+u\frac{\partial T}{\partial x}+v\frac{\partial T}{\partial y}+w\frac{\partial T}{\partial z}=\frac{\partial}{\partial z}\left(K_h\frac{\partial T}{\partial z}\right)+F_T$$

$$\frac{\partial S}{\partial t}+u\frac{\partial S}{\partial x}+v\frac{\partial S}{\partial y}+w\frac{\partial S}{\partial z}=\frac{\partial}{\partial z}\left(K_h\frac{\partial S}{\partial z}\right)+F_S$$

$$\rho=\rho(T,S),$$

where x, y, z are the east, north, and vertical axes in the Cartesian coordinate system; $u, v,$ and w are the x, y, z velocity components; T is the temperature; S is the salinity; ρ is the density; P is the pressure; f is the Coriolis parameter; g is the gravitational acceleration; K_m is the vertical eddy viscosity coefficient; and K_h is the thermal vertical eddy diffusion coefficient. F_u, F_v, F_T and F_S represent the horizontal momentum, thermal, and salt diffusion terms. The total water column depth is $D = H + \zeta$, where H is the bottom depth (relative to $z = 0$) and ζ is the height of the free surface (relative to $z = 0$).

The surface and bottom boundary conditions for temperature are:

$$\frac{\partial T}{\partial z} = \frac{1}{\rho c_P K_h}[Q_n(x,y,t) - SW(x,y,\zeta,t)], \text{ at } z = \zeta(x,y,t)$$

$$\frac{\partial T}{\partial z} = \frac{A_H \tan\alpha}{K_h}\frac{\partial T}{\partial n}, \text{ at } z = -H(x,y),$$

where $Q_n(x,y,t)$ is the surface net heat flux, which consists of four components: downward shortwave, longwave radiation, sensible, and latent fluxes, $SW(x,y,0,t)$ is the shortwave flux incident at the sea surface, and c_P is the specific heat of seawater. A_H is the horizontal thermal diffusion coefficient, α is the slope of the bottom bathymetry, and n is the horizontal coordinate shown in Fig. 6 (Pedlosky, 1974), (Chen et al., 2006).

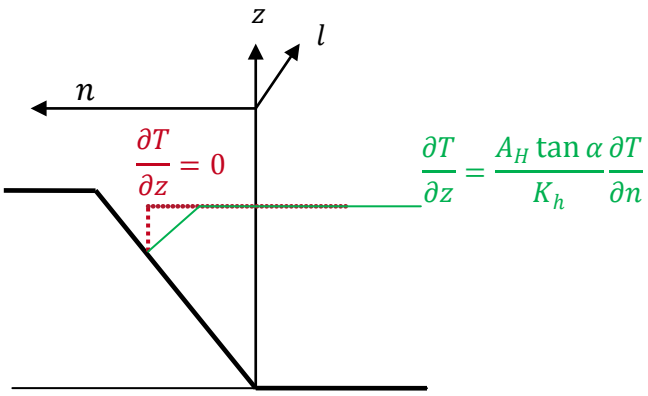

Fig. 6. Schematic of the no-flux boundary condition on the bottom slope

The surface and bottom boundary conditions for salinity are:

$$\frac{\partial S}{\partial z} = -\frac{S(\hat{P}-\hat{E})}{K_h \rho}\cos\gamma, \text{ at } z = \zeta(x,y,t),$$

where $\gamma = \frac{1}{\sqrt{1+|\nabla\zeta|^2}}$

$$\frac{\partial S}{\partial z} = \frac{A_H \tan\alpha}{K_h}\frac{\partial S}{\partial n}, \text{ at } z = -H(x,y),$$

where $\hat{P}$ and $\hat{E}$ are precipitation and evaporation rates, respectively. The groundwater flux can be added into the model by modifying the bottom boundary conditions for vertical velocity and salinity (Chen et al., 2006).

The surface and bottom boundary conditions for $u, v,$ and w are:

$$K_m\left(\frac{\partial u}{\partial z}, \frac{\partial v}{\partial z}\right) = \frac{1}{\rho_0}\left(\tau_{sx}, \tau_{sy}\right), w = \frac{\partial \zeta}{\partial t} + u\frac{\partial \zeta}{\partial x} + v\frac{\partial \zeta}{\partial y} + \frac{E-P}{\rho}, \text{ at } z = \zeta(x, y, t)$$

$$K_m\left(\frac{\partial u}{\partial z}, \frac{\partial v}{\partial z}\right) = \frac{1}{\rho_0}\left(\tau_{bx}, \tau_{by}\right), w = -u\frac{\partial H}{\partial x} - v\frac{\partial H}{\partial y} + \frac{Q_b}{\Omega}, \text{ at } z = -H(x, y),$$

where $\left(\tau_{sx}, \tau_{sy}\right)$ and $\left(\tau_{bx}, \tau_{by}\right) = C_d(u^2 + v^2)(u, v)$ are the *x* and *y* components of surface wind and bottom stresses, Q_b is the groundwater volume flux at the bottom and Ω is the area of the groundwater source. The drag coefficient C_d is determined by matching a logarithmic bottom layer to the model at a height z_{ab} above the bottom (Chen et al., 2006):

$$C_d = \max\left(\frac{k^2}{\ln\left(\frac{z_{ab}}{z_0}\right)^2}, 0.0025\right)$$

where $k = 0.4$ is the von Karman constant and z_0 is the bottom roughness parameter. The kinematic and heat and salt flux conditions on the solid boundary are specified as:

$$v_{\mathrm{n}} = 0;\ \frac{\partial T}{\partial \mathrm{n}} = 0;\ \frac{\partial S}{\partial \mathrm{n}} = 0,$$

where v_{n} is the velocity component normal to the boundary, and n is the coordinate normal to the boundary.

Current research: investigation of different factors impact on the Laptev Sea temperature and salinity distributions using FVCOM

Introduction

The ecosystem dynamics are sensitive to the temperature and salinity variability and thus are connected to the ocean circulation dynamics. Now we are investigating temperature and salinity pattern in the Lena Delta region of the Laptev Sea under the influence of various physical and climate factors in the entire mixed layer over a short period of time in May 2008. The selection of the calculation period was determined by the availability of input data with high quality. In particular the goal is to assess the degree of influence of Lena river runoff temperature, local wind pattern and tides dynamics on temperature and salinity variability in the considered area. In addition the attention is paid to assessment of the impact of local bathymetry on local temperature and salinity patterns.

Due to short modeling period we did not take into account the freshening by ice melting. The fast-ice in the Laptev Sea, in particular in Lena Delta region, generally, breaks up when freshwater runoff reaches its maximum (Bauch et al., 2009). For the last 100 years a tendency towards earlier daily maximum flow formation was observed (Fig. 7). For example, in 2008 the daily maximum flow formed at the end of May.

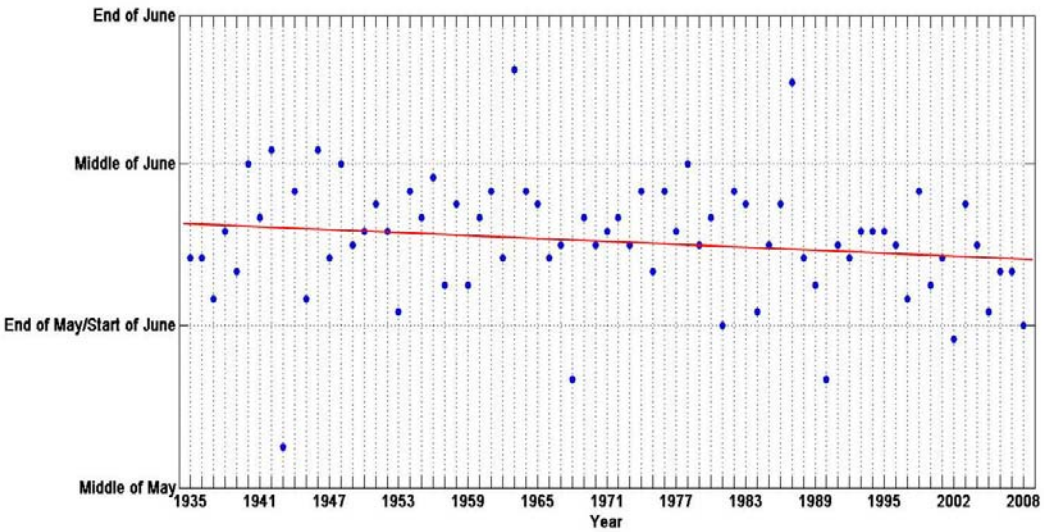

Fig. 7. The time of the year when the daily flow of Lena reaches a maximum. The regression line is showed in red. The theoretical slope of the line is significantly different from 0 at the 18% level.

Satellite images (Sascha Willmes, Trier University) show that during May 2008, drifting and fast ice occupy almost the whole region of the Laptev Sea except the western New Siberian polynya and Anabar-Lena polynya zones. The polynya activity in the winter season 2007/2008 was much lower than in 2006/2007 (Willmes et al., 2011). We can assume that during May 2008 a thin layer of ice preserved in the considered domain, except the zone of polynyas. In that case we can study under-ice layers considering presence of ice thin layer in heat exchange with the atmosphere and temperature field. We do not take into account the changes in wind momentum transfer due to presence of ice. However the wind velocity magnitudes for entire calculation period for the model were small (the magnitudes maximum is 6.3 m/s).

Interannual river discharge variability can also influence to local interannual salinity and temperature variations. However, the role of discharge variability for all Siberian rivers at this stage is estimated to be negligible (Berezovskaya et al., 2002)(Steele, 2004)(Dmitrenko et al., 2005). For the local modeling with a small spatial scale this result may not be entirely true. Freshwater runoff in the model is implemented across the entire width of the Lena mouth (more than 400 km), where three main freshwater channels (Trofimovskaya, Bykovskaya Olenekskaya ducts) are situated (Magritsky, 2001) (Fig. 8), and the modeling time interval is less than one month.

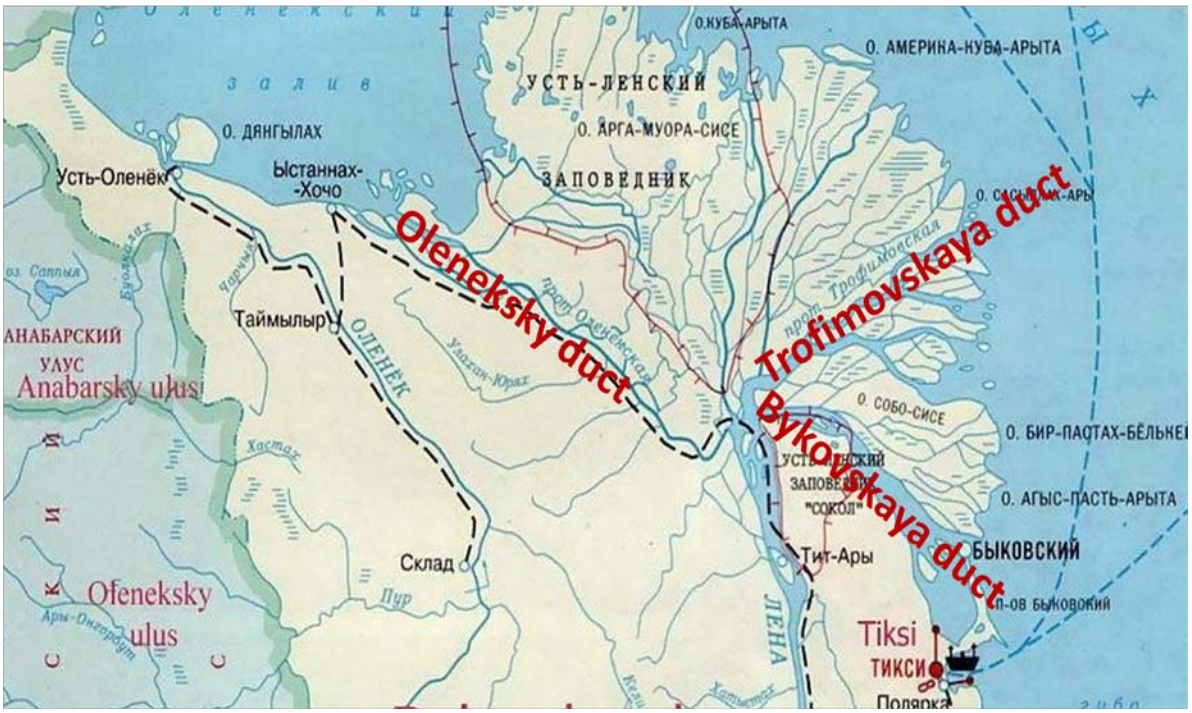

Fig. 8. The schematic sketch of main ducts of the Lena River.

For this reasons we did not take into account the discharge variability in this work. Also precipitation and evaporation were not part of our analysis.

Methods and data

The first step was to choose a part of the Laptev Sea avoiding amphidromes on the open boundary and large enough to trace the distribution of fresh water. This step was based on tidal map (Sof'ina, 2008), satellites images provided by (Sacha Willems, Trier University; Thomas Krumpen, Alfred Wegener Institute (Bremerhaven); Birgit Heim, Alfred Wegener Institute (Potsdam)) respectively. Then we compared GEBCO (The General Bathymetric Chart of the Oceans) bathymetry data (GEBCO, web source) with 1 km and NOAA (The National Oceanic and Atmospheric Administration) coastline data with 5 km resolution (NOAA, web source) and constructed coastline with 1 km resolution. To smooth the coastline we used cubic b-splines technique.

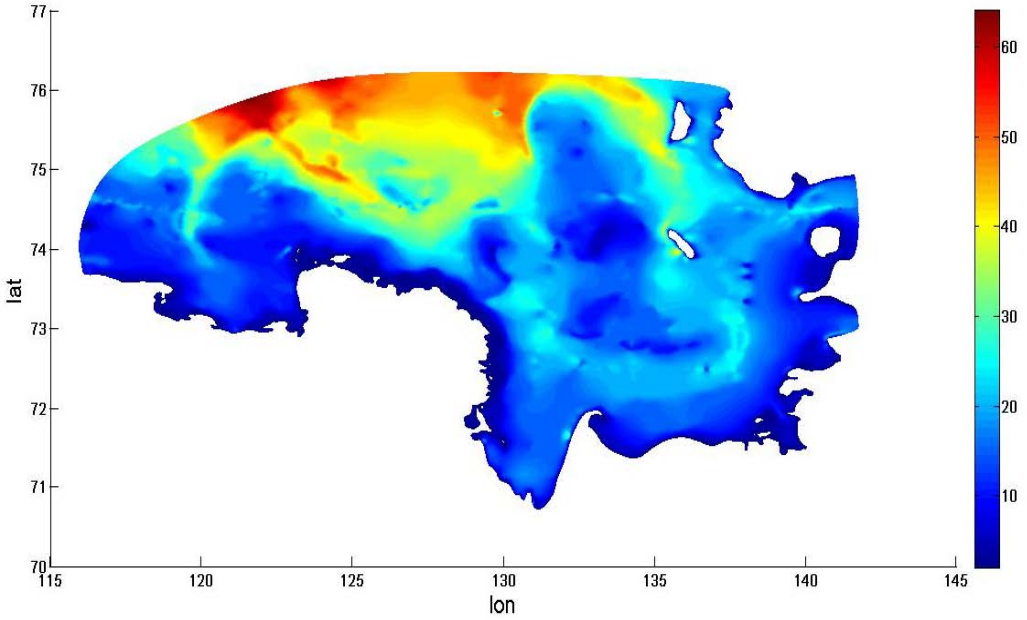

Fig. 9. Bathymetry data in the selected domain (GEBKO, resolution ~ 1 km), m.

The second step was to obtain a high quality unstructured grid allowing us to take into account the complexity of coastline and bathymetry as well as other features of the problem (for example, the necessity to reduce the size of elements on a main directions of Lena fresh water plume propagation). For this purposes we implemented Persson's algorithm (Persson, Strang, web source). The element size function was constructed based on bathymetry and its gradient. Element sizes vary from 400m to 3 km. The model contains seven vertical levels (six sigma-layers (Chen et al., 2006)) with 250000 nodes on each of them.

The third step was to select input data appropriate to our task. The wind magnitudes and direction, radiation fluxes were taken from the regional, non-hydrostatic model provided by the consortium for Small-scale Modeling (COSMO). The time resolution for

atmospheric forcing is 1 hour. The COSMO model with included thermodynamic sea-ice module provides a high quality atmospheric forcing allowing to take into account the presence of a thin layer of ice and can be applied for short-range simulations (Steppeler et al., 2003), (Schättler et al.), (Schröder et al., 2011). Sea ice derives from AMSR-E (The Advanced Microwave Scanning Radiometer - EOS) Sea ice concentration (SIC) data. The ice thickness is set to 1m at positions where AMSR-E SIC is above 70% (Schröder et al., 2011). We used results from COSMO simulations with 5 km resolution performed for the Laptev Sea area with and without assumption that the Laptev Sea polynyas are ice-free (positions where AMSR-E SIC is below 70% are set to 0 cm and 10 cm ice respectively). For these COSMO simulations boundary conditions have been taken from the COSMO simulations with 15 km resolution (initialized by GME analysis). The FESOM Laptev Sea polynya dynamics simulations with forcing provided by COSMO are closer to AMSR-E compared simulations with 6-hourly NCEP (National Centers for Environmental Prediction) reanalysis 1 (1.875° _ 1.875°), 6-hourly NCEP reanalysis 2 (1.875° _ 1.875°), 6-hourly analyses from the GME (Global Model of the German Weather Service) (0.5° _ 0.5°) (Ernsdorf et al., 2011).

The temperature and salinity fields for initializing the model (Fig. 10) and for daily nudging on the open boundary were taken from Arctic simulations by Rüdiger Gerdes and Polona Rozman with focus on the Laptev Sea region (Rozman et al., 2011). This model provides data, which are in a good agreement with long-term mean (1920-2008) surface salinity distribution for winter season (February-April) described in (Dmitrenko et al., 2010a) and salinity observation data for May 2008 (Markus Janout, Alfred Wegener Institute (Bremerhaven)). Also, the provided salinity/temperature patterns are close to the pattern of seasonal cycle from summer 2007 to late winter/spring of 2008 shown in (Hölemann et al., 2011). This sea-ice model provides daily data for temperature and salinity field in the region for 6 vertical layers.

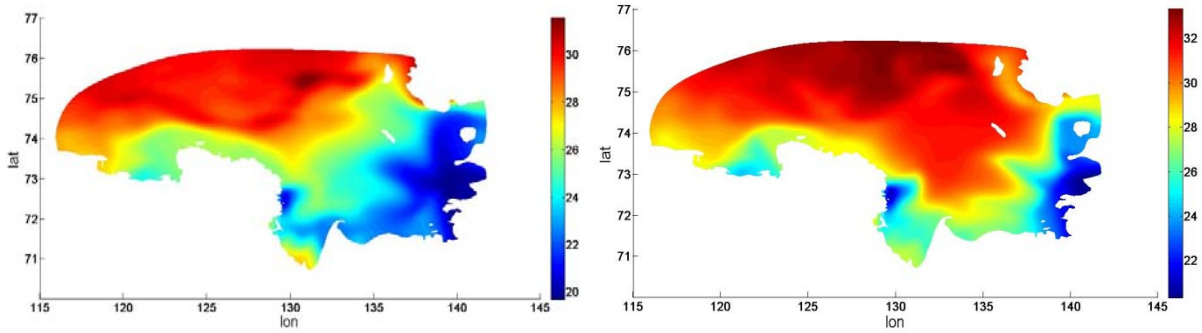

a) **b)**

Fig. 10. Initial of salinity fields (9 of May, 2008 at 00:00:00), PSU, in
a) surface layer b) bottom layer

The tidal components were taken from TPXO6.2 with Doodson's correction. The model simulates the four most energetic tidal constituents: (Sof'ina, 2008), (Lenn et al., 2011), (Kowalik, 1993).

The input daily Lena runoff data, derived from observations, were provided by Hydrological Institute, St. Petersburg. The runoff temperature was set to either 0.5 °C or 5°C, which present, respectively, the approximately lower and upper bounds for mean temperature in the river mouth during May based on (Yang et al., 2002), (Yang et al., 2005), (Costard et al., 2007). For assessment of the influence of local bathymetry on temperature and salinity patterns we used additionally bathymetry measurement data in Lena Delta region (Paul Overduin, Alfred Wegener Institute, Potsdam).

We used two techniques to distribute of total volume runoff. In the first case the freshwater input was realized only from the Lena Delta boundary depending on spatial runoff structure, which is described in (Magritsky, 2001). In the second case, the freshwater input was distributed in some vicinity of Lena Delta depending not only on spatial runoff structure, but on the measured depth too. The second technique allowed us to avoid anomalous water elevation in Lena Delta zone (maximum of runoff in 2008 was observed at the end of May), to form the main freshwater channels and estimate the degree of influence of bathymetry data.

The FVCOM was compiled and run with following properties:

- Use spherical coordinates
- Include wet/dry treatment of domain
- Use GOTM turbulence model
- Use open boundary Temperature/Salinity time series nudging
- External time step is 6 sec, ratio of internal mode time step to external mode time step is 10

Wind pattern in the considered domain in May 2008

Based on atmospheric data COSMO a very unstable and heterogeneous wind pattern was observed in May 2008 in comparison, for example, with May 2009. The atmospheric circulation patterns in the west and east parts of model domain were often sharply different. The invasion of powerful winds from the continent often caused a ring-bark atmospheric circulation around Lena Delta from west to east as well as from east to west. As a result of strong northward winds in the eastern part of the domain, and weaker south-eastward winds in the western part a counterclockwise vortex was observed at least 5 times in May in the northern vicinity of the Lena Delta (Fig. 11), which persisted for more than 12 hours while moving northeast, a counterclockwise vortex was also once observed near Tiksi bay. A reverse situation is also observed, albeit rarely and mostly at the end of the month - clockwise vortex, due to strong northward winds in the western part of the domain.

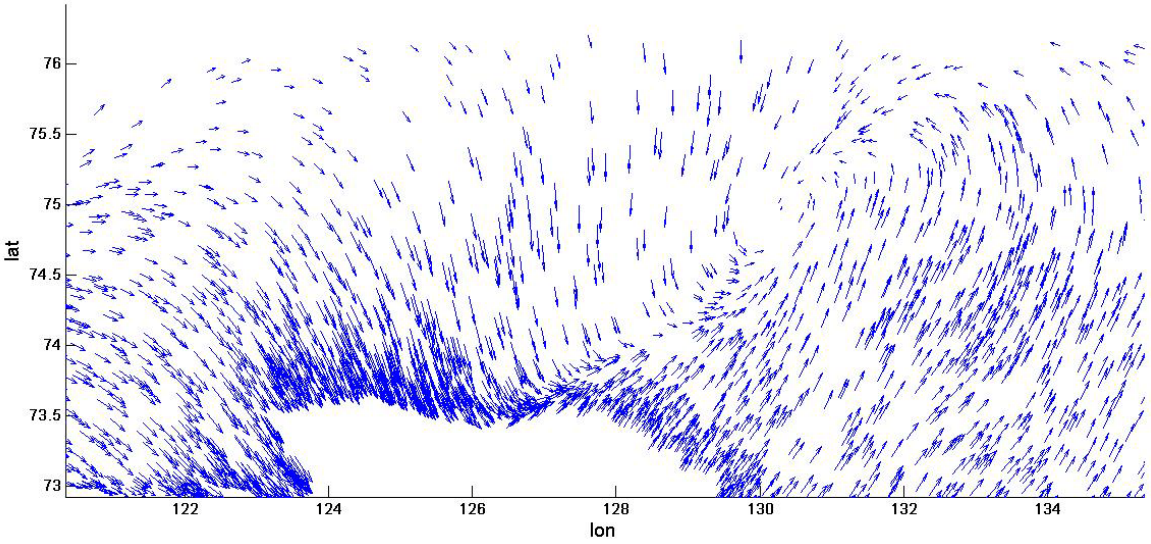

Fig. 11. The counterclockwise vortex in the wind velocity in north-eastern part of the Lena Delta, the velocity vectors are shown every 100th point of an unstructured grid.

In general, dominated locking westward (Fig. 12) and rarely locking eastward winds and on-shore northward winds (except for the first days of month and several days in the middle of month). The maximum wind speed in May 2008 according to COSMO simulations in this domain reached 6.3 m/s, the minimum - 1.9 m / s and the average speed for the period amounted to 4.06 m/s. This wind speed range is broadly in line with the norms of the region's climate. In the late spring and summer winds are prevailing with speeds not exceeding 3-4 m/sec. The powerful winds with speed more than 20m/sec are not observed in the summer (Dobrovolsky, Zalogin, 1982).

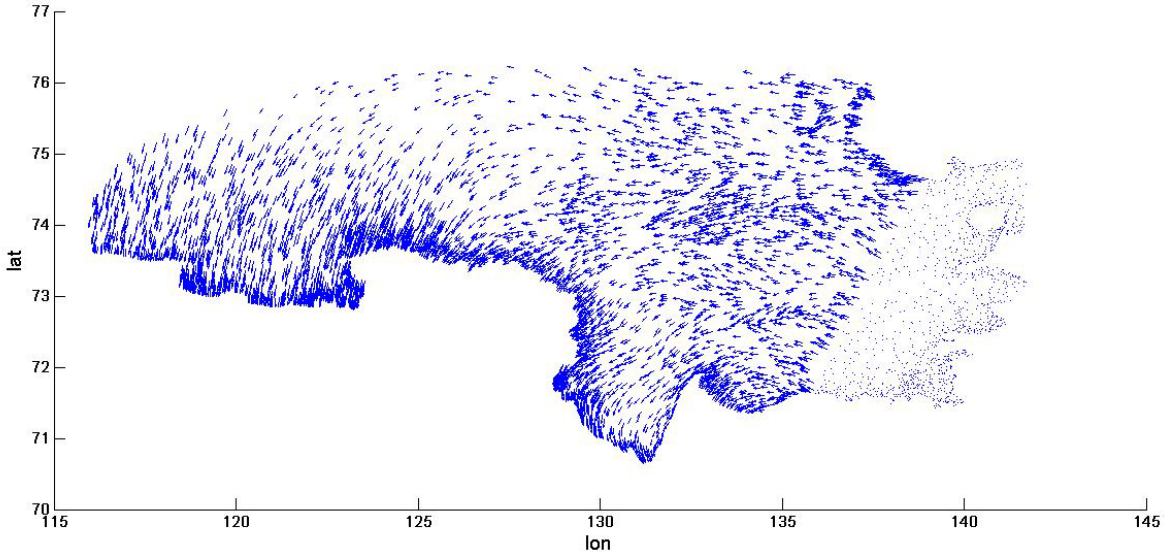

Fig. 12. The locking westward winds (ring-bark circulation around Lena Delta), the velocity vectors are shown every 100th point of an unstructed grid, zeros in the eastern zone is the area without wind information (in model we used nearest interpolation).

Results

We compare salinity and temperature fields in mixed layer under the ice in simulations with and without atmospheric forcing, tidal dynamics, with different temperatures of freshwater and techniques of freshwater input. The table below matches different cases with the resulting figures.

Figure	Atmospheric forcing (COSMO data)		Tidal dynamic	Boundary runoff	Distributed runoff	Runoff temperature, °C
	Open polynya assumption	No open polynya assumption				
Fig. 13a), Fig16a)		+	+	+	-	0.5
Fig. 15a)		+	+	-	+	0.5
Fig. 13b)	-		+	+	-	0.5
Fig. 15b)	-		+	-	+	0.5
Fig. 13c)		+	-	+	-	0.5
Fig. 16b)	+		+	+	-	0.5
Fig. 16c)	+		+	+	-	5

From the results of numerical simulations very heterogeneous, with vorticity map of currents is formed in May 2008 in the selected domain. This situation results from local wind pattern and complexity of coastline. In conformity with the characters of wind pattern we received lock riverine water in the vicinity of the Lena Delta and also desalination of northern part of the vicinity.

The surface salinity and temperature fields in the central part of the Laptev Sea (the northern and eastern vicinity of Lena Delta) are mainly determined by the local wind pattern. Note that the locking westward winds lead in mouth zone of Lena the freshwater distribution to the east in the western part and to the north in the northern part of Lena Delta vicinity, the locking eastward winds lead nailed flows to mouth due to the Coriolis force.

The characteristics of the tidal dynamics in the region also have an important role in local salinity and temperature distributions. The salinity and temperature insensitivity to atmospheric circulation over the shelf east of the Lena Delta over the whole mixed layer, is explained, according to the model, by the Coriolis forcing and the nature of the tidal dynamics in the region. These forces play main role in this area due to nearby presence

of the largest freshwater ducts. Also tides play significant role in water mass modification, turbulence, and vertical mixed of seawater properties across the mixed layer.

The variability of runoff temperature influences only little the freshwater plume direction. However, the heat fluxes structure greatly affects the temperature pattern variability in the entire mixed layer.

In studies local temperature and salinity patterns, because of small wind velocity in the region, the detailed representation of freshwater channels and distribution of total runoff volume over these channels becomes particularly important. Also we should emphasize the particular importance of the coastline detail in case of boundary runoff.

Discussion

In the north and west vicinity of the Delta the freshening is mainly affected by wind pattern (Fig. 13a). This result is consistent with the results outlined in (Dmitrenko et al., 2005), (Dmitrenko et al., 2010a). However the salinity and temperature fields are invariant of atmospheric circulation over the shelf east of the Lena Delta, this fact is noted in background hydrography in (Dmitrenko et al., 2010a). For all 3 panels of Fig.13 we observed a freshcurrent along the shoreline to the right of the Lena Delta. This effect is explained by the Coriolis force and the location of the main ducts. The Trofimovskaya duct (dumps into the Sea on the average 62% of river water) is situated north of Bykovskaya (dumps into the Sea on the average 25% of river water), in the east part of Lena Delta (Fig. 15).

The powerful freshwater stream of Trofimovskaya duct has a pronounced southern direction due to the Coriolis force and leads the freshwater from Bykovskaya duct. The same dynamic was observed for every depth layer. In this case the local wind pattern with small magnitudes of velocities turns out to be of no relevance, which leads to salinity and temperature fields' insensitivity to atmospheric circulation over the shelf area east of the Lena Delta in flooding period. In the given work the situation was complicated since the maximum daily flow in 2008 occurred in late May, within the period of simulations. The land-fast ice can also reduce the impact of wind to surface hydrography (Dmitrenko et al., 2010a) that increases the role of Coriolis forcing in freshening of shoreline zone to the east of Lena Delta.

The dissipation of tidal energy also plays significant role in water mass modification and vertical mixed of seawater (Fig. 13), this fact has been well described for continental shelf seas (Simpson et al. , 1996) (Lenn et al., 2011). Also estimates by (Dmitrenko et al., 2012) of the gradient Richardson numbers from the April-May 2008 observations over the eastern Laptev Sea shelf (~74°N, 128 °E) provided evidence that the velocity shear associated with semidiurnal baroclinic tidal flow may be strong enough to play a role in water mass modification, promoting shear instabilities, turbulence, and vertical mixed of seawater properties across the shelf halocline layer. In the southeast part of the Lena Delta vicinity the powerful freshwater stream from the largest freshwater Lena's ducts - Trofimovskaya and Bykovskaya, forms the velocity magnitude gradients for every depths layer with directions corresponding to the tidal ellipses of the region (Fig. 13a,b). The tidal ellipse of barotropic velocity (vertical averaged) in the eastern vicinity of Lena Delta have counterclockwise direction (Sof'ina, 2008).

The pronounced cyclonic atmospheric circulation in late spring/summer season (for example, in 2007) may strengthen the freshening effect over the shelf east of the Lena Delta. It should lead the appearance of big temperature and salinity anomalies compared

to the climatic mean. This conclusion correlates with the expeditions data of 2007 (AARI, web source).

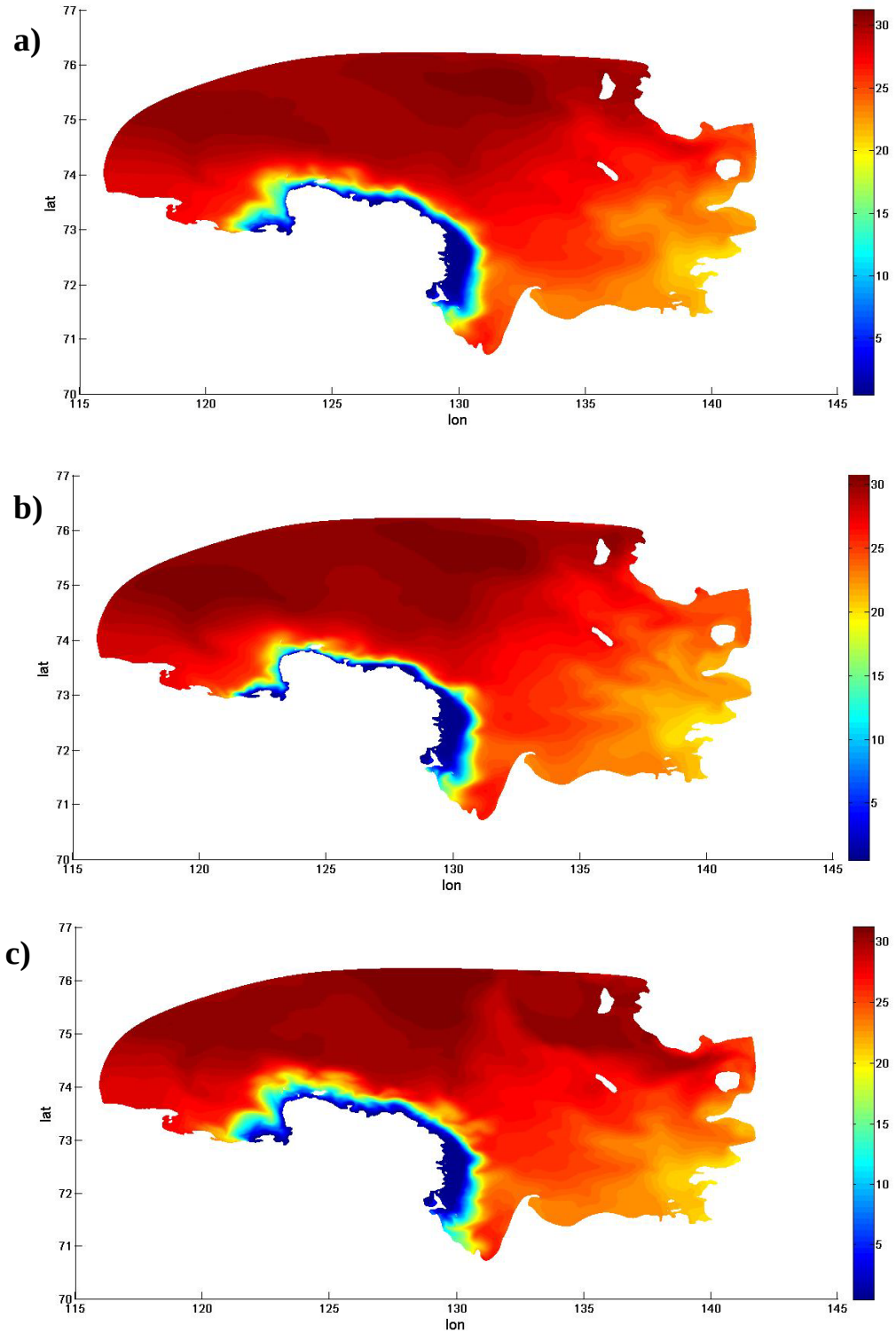

Fig. 13. The salinity fields, freshwater runoff input from the boundary, calculation period - 22.234583 days from 9 of May 2008 to 31 of May 2008, PSU: a) atmospheric forcing from COSMO without open polynya's assumption, b) no atmospheric forcing, c) atmospheric forcing is the same as in a), but no tidal dynamics.

Additionally we simulated cases with increased discharge rate by a factor of 20. The results of these simulations confirmed the importance of runoff structure and tidal dynamics characteristics for temperature and salinity patterns analysis in the region (Fig. 14a,b).

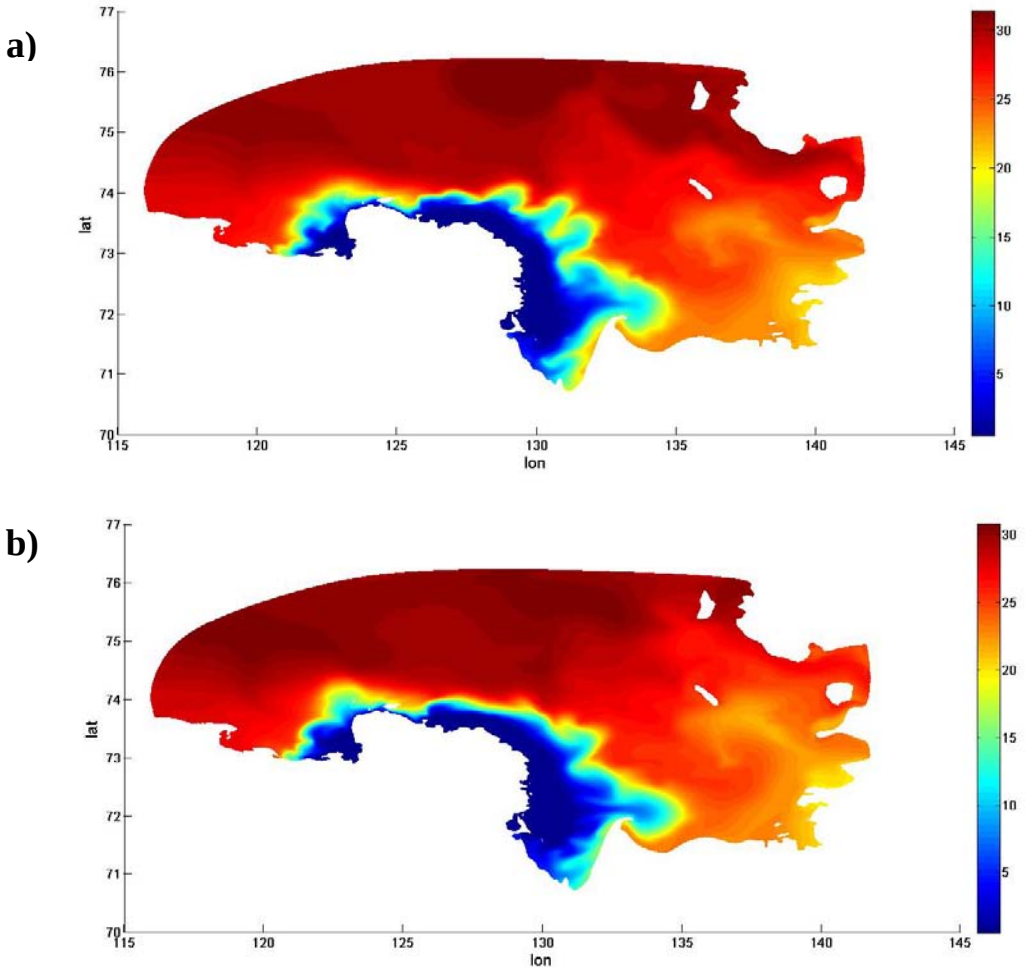

Fig. 14. The salinity fields, freshwater runoff input from the boundary with increased discharge rate in 20 times, calculation period - 16.93447917 days from 9 of May 2008 to 25 of May 2008, PSU: a) atmospheric forcing from COSMO without open polynya's assumption, b) no atmospheric forcing.

In the case of the distributed runoff (Fig. 15), we receive accurate created freshwater channels and more precise vertical stratification in vicinity zone. In general, we observed similar behavior in both cases (with and without detailed elaboration of freshwater channels). It should be noted that in both boundary and distributed runoff cases we used the same structure of volume runoff distribution. The picture is sharply different for an arbitrary runoff volume distribution. The formation only one freshwater channel or using small amount of nodes/edges for freshwater input in the model can lead to significant

errors in local salinity and temperature pattern in flooding period of Lena, even when using small (less than 1 minute) time step for runoff input. Also errors in coastline topography can lead to significant changing in local temperature and salinity distribution when using runoff from the boundary. The wind pattern can be neglected in the whole vicinity of Lena Delta in contrast to tidal dynamics and coastal topography, due to anomaly gradient of elevation and velocity magnitude in runoff zone in the model.

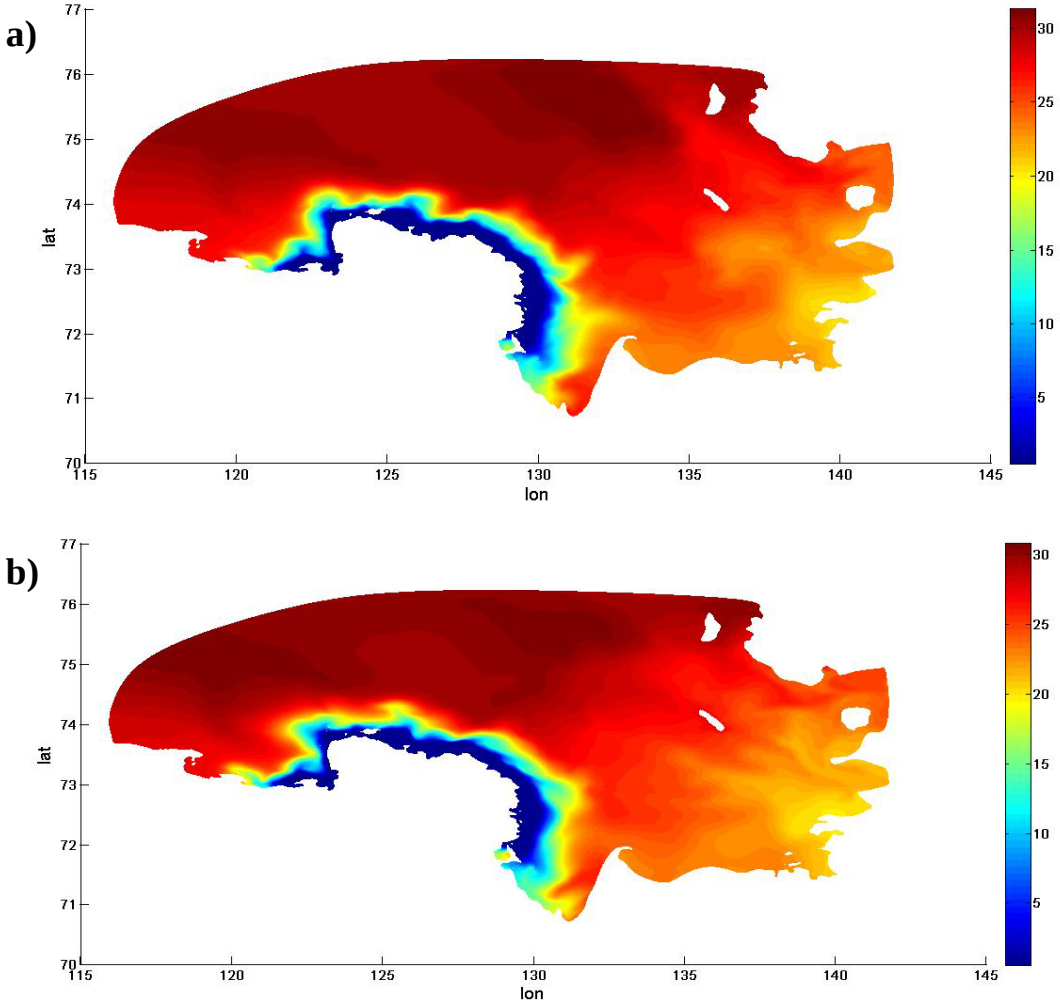

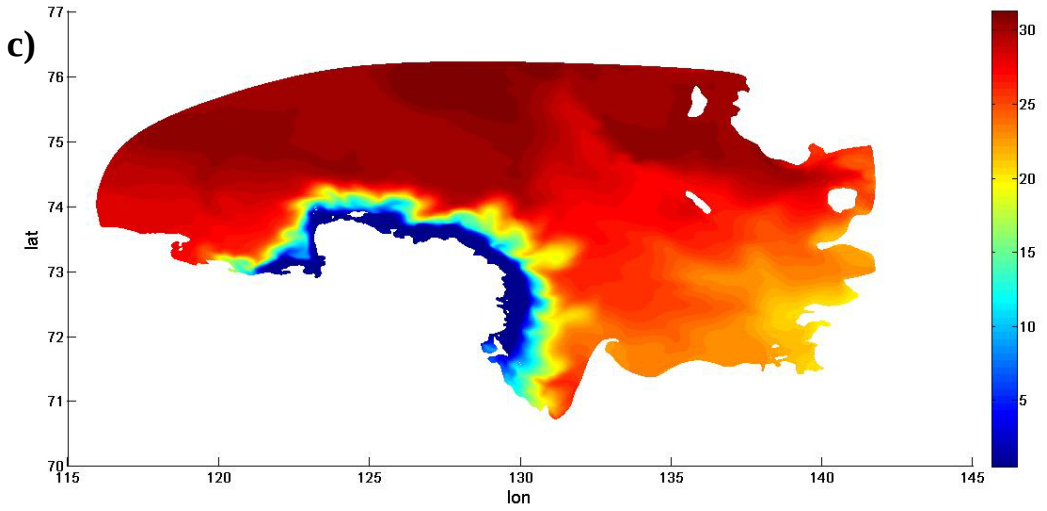

Fig. 15. The salinity fields, freshwater runoff input from the vicinity with detailed elaboration of freshwater channel, calculation period – 18.5633 days from 9 of May 2008 to 27 of May 2008, PSU: a) atmospheric forcing from COSMO without open polynya assumption, b) no atmospheric forcing, c) atmospheric forcing from COSMO without open polynya assumption, no tidal dynamics.

The changes in structure of heat fluxes (COSMO data with and without open polynya's assumption) and in runoff temperature do not significantly influence the propagation of freshwater plume. However these changes effect a lot to temperature pattern in the region in whole mixed layer (Fig. 16). These results are in an agreement with (Hölemann et al., 2011), (Ebner et al., 2011).

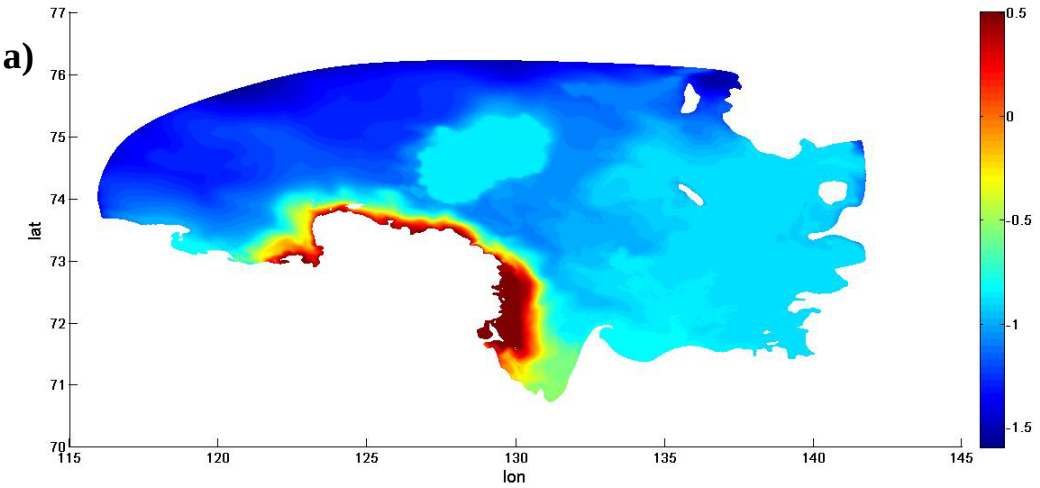

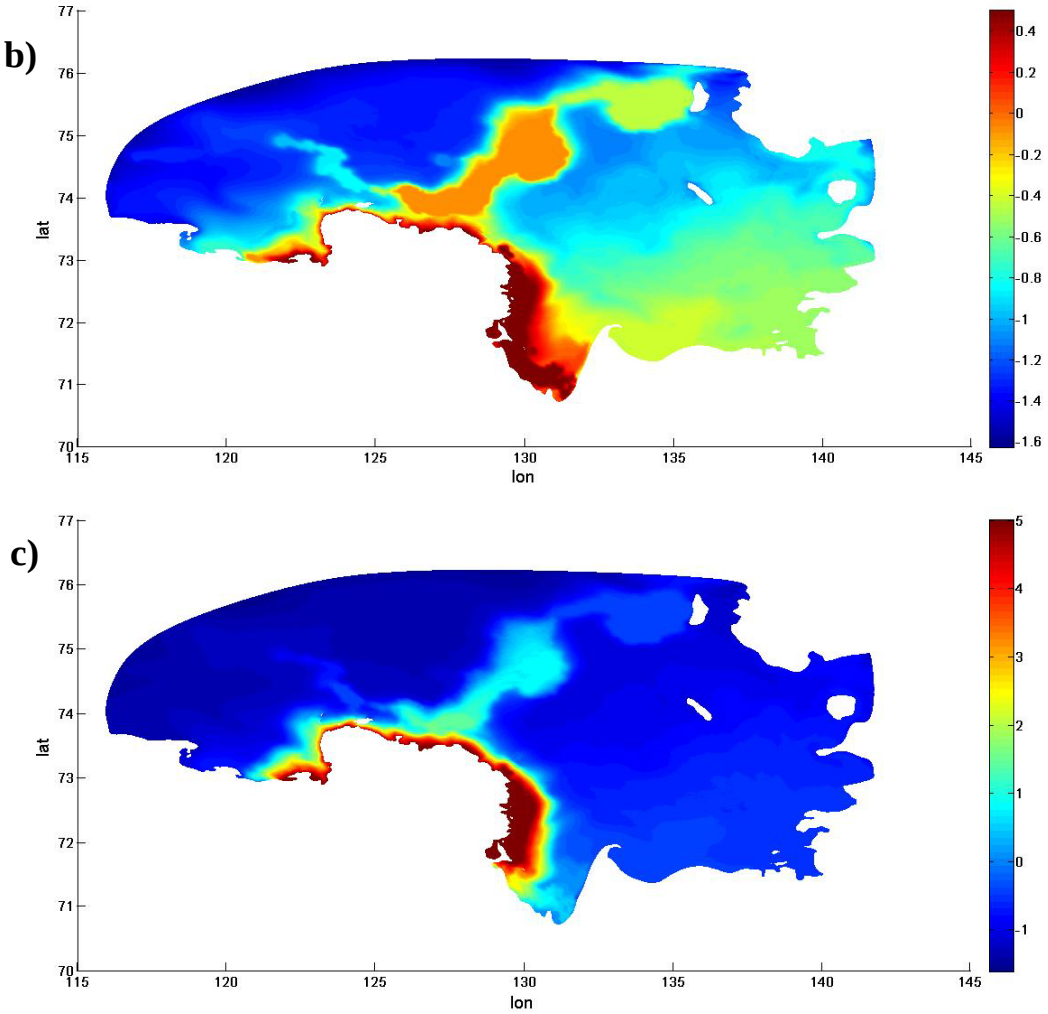

Fig. 16. The temperature fields, freshwater runoff input from the boundary with increased discharge rate in 20 times, calculation period - 22.234583 days from 9 of May 2008 to 31 of May 2008, the wind pattern is the same for all simulations, °C: a) atmospheric forcing from COSMO without open polynya's assumption, runoff temperature is 0.5 °C, b) atmospheric forcing from COSMO with open polynya's assumption, runoff temperature is 0.5 °C, c) atmospheric forcing from COSMO with open polynya's assumption, runoff temperature is 5 °C.

Time table

Work package	2011/2012 Sub package											
	Sep	Oct	Nov	Dec	Jan	Feb	Mar	Apr	May	Jun	Jul	Aug
Running baroclinic case base on FVCOM (The Unstructured Grid Finite Volume Coastal Ocean Model) for Lena Delta region of the Laptev sea during one month in late spring/summer period	Reviewing of relevant literature											
	Choice of the domain under consideration and creating unstructured grid with high quality											
	Simulation of barotropic case base on FVCOM											
	Simulation of baroclinic case base on FVCOM											
	Investigation of temperature and salinity pattern in the Lena Delta region of the Laptev Sea under the influence of various physical and climate factors in the entire mixed layer over a short period time in May 2008, writing article											
Work package	2012/2013 Sub package											
	Sep	Oct	Nov	Dec	Jan	Feb	Mar	Apr	May	Jun	Jul	Aug
Implemented of ice module	Implemented of ice module, test simulation											
	Comparing with observations data											

German course												
Assimilation data task												
Tidal Dynamic Analysis according to ice mask, writing article												
Trip to Russia, comparing numerical results												
Bottom permafrost changing and vertical stratification analysis, writing article												
Implemented bio-module (passive mixture)												
TOC analysis, primary production analysis												
Expedition to Lena Delta region												
Work package	2013/2014											

	Sub package											
	Sep	Oct	Nov	Dec	Jan	Feb	Mar	Apr	May	Jun	Jul	Aug
Data analysis												
Real time model running												
Writing PhD thesis, writing article												

References

1. "Arctic and Antarctic Research Institute" Federal State Budgetary Institution, The current state and variability of the natural environment of the Laptev Sea region as a reflection of global climate processes. http://portalrp.ru/atmosphere-and-hydrosphere-monitoring-2007-2010-projects/tech-02-515-11-5080 Last accessed: 30.07.2012 (in Russian).

2. Alexandrov, V.Y., Martin, T., Kolatschek, J., Eicken, H., Kreyscher, M., Makshtas, A.P., 2000. Sea ice circulation in the Laptev Sea and ice export to the Arctic Ocean: Results from satellite remote sensing and numerical modeling. Journal of Geophysical Research 105 (C5), 17143–17159. doi:10.1029/2000JC900029.

3. Bauch, D., Dmitrenko, I., Kirillov, S., Wegner, C., Hölemann, J., Pivovarov, S., Timokhov, L., Kassens, H., 2009. Eurasian Arctic shelf hydrography: Exchange and residence time of southern Laptev Sea waters. Continental Shelf Research 29 (15), 1815-1820, doi:10.1016/j.csr.2009.06.009.

4. Bareiss, J., Goergen, K., 2005. Spatial and temporal variability of sea ice in the Laptev Sea: analysis and review of satellite passiv-microwave data and model results, 1997 to 2002. Global Planet. Change 48, 28–54.

5. Berezovskaya, S. L., Dmitrenko, I. A., Gribanov, V. A., Kirillov, S. A., Kassens H., 2002. Distribution of river waters over the Laptev Sea shelf under different atmospheric circulation conditions. Doklady Earth Sciences 386(7), 804 – 808.

6. Chen, C., Beardsley, R.C., Cowles, G., 2006. An Unstructured Grid, Finite-Volume Coastal Ocean Model. FVCOM User Manual, second ed. SMAST/UMASSD-06-0602.

7. Chen, C., Liu, H., Beardsley, R. C., 2003. An Unstructured Grid, Finite-Volume, Three-Dimensional, Primitive Equations Ocean Model: Application to Coastal Ocean and Estuaries. Journal of Atmospheric and Oceanic Technology 20(1), 159, doi: 10.1175/1520-0426(2003)020<0159:AUGFVT>2.0.CO;2

8. Comiso, J. C., 2010. Variability and Trends of the Arctic Sea Ice Cover. Sea Ice 2, Wiley-Blackwell, New York, US, 2010.

9. Costard, F., Gautier, E., Brunstein, D., Hammadi, J., Fedorov, A., Yang, D., Dupeyrat, L., 2007. Impact of the global warming on the fluvial thermal erosion over the Lena River in Central Siberia. Geophys. Res. Lett. 34, L14501, doi:10.1029/2007GL030212.

10. Dethleff, D., Loewe, P., Kline, E., 1998. The Laptev Sea flaw lead – detailed investigation on ice formation and export during 1991/1992 winter season. Cold Reg. Sci. Technol. 27, 225–243.

11. Dmitrenko, I., Kirillov, S., Eicken, H., Markova, N., 2005. Wind-driven summer surface hydrography of the eastern Siberian shelf. Geophysical ReSearch Letters 32, L14613.

12. Dmitrenko, I. A., S. A. Kirillov, and L. B. Tremblay, 2008a. The long-term and interannual variability of summer fresh water storage over the eastern Siberian shelf: Implication for climatic change. J. Geophys. Res. 113, C03007, doi:10.1029/2007JC004304.
13. Dmitrenko, I. A., Kirillov, S. A., Ivanov, V. V., Woodgate, R. A., 2008b. Mesoscale Atlantic water eddy off the Laptev Sea continental slope carries the signature of upstream interaction. J. Geophys. Res. 113, C07005, doi:10.1029/2007JC004491.
14. Dmitrenko, I. A., Kirillov, S. A., Krumpen, T., Makhotin, M., Abrahamsen, E. P., Willmes, S., Bloshkina, E., Hölemann, J. A., Kassens, H., Wegner, C., 2010a. Wind-driven diversion of summer river runoff preconditions the Laptev Sea coastal polynya hydrography: Evidence from summer-to-winter hydrographic records of 2007–2009. Continental Shelf Research 30(15), 1656-1664.
15. Dmitrenko, I. A. , Kiriilov, S. A. , Tremblay, L. B. , Bauch, D. , Hölemann, J. , Krumpen, T. , Kassens, H. , Wegener, C. , Heinemann, G., Schröder, D., 2010b. Impact of the Arctic Ocean Atlantic water layer on Siberian shelf hydrography. Journal of Geophysical Research 115, C08010, doi: 10.1029/2009JC006020.
16. Dmitrenko, I. A., Kirillov, S. A., Bloshkina, E., Lenn, Y.D., 2012. Tide-induced vertical mixed in the Laptev Sea coastal polynya, J. Geophys. Res. 117, doi:10.1029/2011JC006966.
17. Dobrovolsky, A. D., Zalogin, B. S., 1982. The Seas of the U.S.S.R. Lomonosov Moscow State University Press (in Russian).
18. Ebner, L., Schröder, D., Heinemann, G., 2011. Impact of Laptev Sea flaw polynyas on the atmospheric boundary layer and ice production using idealized mesoscale simulations. Polar Research 30, 7210, doi:10.3402/polar.v30i0.7210.
19. Eicken, H., Dmitrenko, I. A., Tyshko, K., Darovskikh, A., Dierking,W., Blahak, U., Groves, J., Kassens, H, 2005. Zonation of the Laptev Sea landfast ice cover and its importance in a frozen estuary. Global Planet. Change 48, 55–83.
20. Ernsdorf, T., Schröder, D., Adams, S., Heinemann, G., Timmermann, R., Danilov, S., 2011. Impact of atmospheric forcing data on simulations of the Laptev Sea polynya dynamics using the Sea-ice ocean model FESOM. J. Geophys. Res., 116, C12038, doi:10.1029/2010JC006725.
21. GEBCO. http://www.gebco.net/data_and_products/gridded_bathymetry_data/ Last accessed: 30.07.2012
22. Hölemann, J., Kirillov, S., Klagge, T., Novikhin, A., Kassens, H., Timokhov, L., 2011. Near-bottom water warming in the Laptev Sea in response to atmospheric and sea ice conditions in 2007. Polar Research 30, doi: 10.3402/polar.v30i0.6425.
23. Johnson, M.A., Polyakov, I., 2001. The Laptev Sea as a source for recent Arctic Ocean salinity change. Geophysical ReSearch Letters 28 (10), 2017–2020.

24. Kotyukh, A.A., Kluyev, Ye.V., Morozov, B.N., 1990. Repeated depth measurements - main source to find out the change of the bottom topography of the Laptev Sea in the current epoch. Vestnik of the Leningrad University, ser. geology and geography, ser.7 (3), pp.53060
25. Kowalik, Z., Proshutinsky, A. Y., 1993. Diurnal Tides in the Arctic Ocean, J. Geophys. Res. 98(C9), 16,449–16,468, doi:10.1029/93JC01363.
26. Kowalik, Z., Proshutinsky, A. Y., 1994. The Arctic Ocean tides, in: Johannessen, O. M., Muench, R. D., Overland, J. E., The Polar Oceans and Their Role in Shaping the Global Environment, Geophys. Monogr. Ser. 85, 137–158, AGU, Washington, D. C., doi:10.1029/GM085p0137.
27. Kwok, R., G. F. Cunningham, W. D., Hibler III, 2003. Sub-daily sea ice motion and deformation from RADARSAT observations. Geophys. Res. Lett. 30, 2218, doi:10.1029/2003GL018723.
28. Kwok, R. and Rothrock, D. A., 2009. Decline in Arctic sea ice thickness from submarine and ICESat records: 1958–2008. Geophys. Res. Lett., 36, L15501, doi:10.1029/2009GL039035.
29. Lenn, Y. D., Rippeth, T. P., Old, C. P., Bacon, S., Polyakov, I., Ivanov, V., Hölemann, J., 2011. Intermittent Intense Turbulent Mixed under Ice in the Laptev Sea Continental Shelf. Journal of Physical Oceanography 41 (3), 531-547, doi:10.1175/2010JPO4425.1.
30. Magritsky, D. V., 2001. The natural and anthropogenic changes in the hydrological regime of the lower reaches and estuaries of major rivers of Eastern Siberia. Dissertation, Lomonosov Moscow State University (in Russian).
31. Meier, W. N., Stroeve, J., and Fetterer, F., 2007. Whither Arctic sea ice? A clear signal of decline regionally, seasonally and extending beyond the satellite record. Ann. Glaciol. 46, 428–434, doi:10.3189/172756407782871170.
32. NOAA. http://www.ngdc.noaa.gov/mgg/shorelines/shorelines.html Last accessed: 30.07.2012
33. Persson, P.O., Strang, G., A simple mesh generator in MATLAB. http://persson.berkeley.edu/distmesh/persson04mesh.pdf Last accessed: 30.07.2012
34. Pnyushkov, A.V., Polyakov, I.V., 2011. Observations of Tidally Induced Currents over the Continental Slope of the Laptev Sea. Arctic Ocean
35. Polyakov, I.V., Alexeev, V.A., Belchansky, G.I., Dmitrenko, I.A., Ivanov, V.V., Kirillov, S.A., Korablev, A.A., Steele, M., Timokhov, L.A., Yashayaev, I., 2008. Arctic Ocean freshwater changes over the past 100 years and their causes. Journal of Climate 21 (2), 364–384.

36. Proshutinsky, A., Timmermans, M.-L., Ashik, I., Beszczynska-Moeller, A., Carmack, E., Eert, J., Frolov, I., Itoh, M., Kikuchi, T., Krishfield, R., McLaughlin, F., Rabe, B., Schauer, U., Shimada, K., Sokolov, V., Steele, M. , Toole, J., Williams, W., Woodgate, R., Zimmermann, S., 2011. Arctic Report Card: update for 2011, Ocean, http://www.arctic.noaa.gov/reportcard/ocean.html Last accessed: 30.07.2012
37. Rigor, I. G., Colony, R. L., 1997. Sea-ice production and transport of pollutants in the Laptev Sea, 1997–1993. Sci. Total Environ. 202, 89–110.
38. Romanov, I. P. Atlas of Ice and Snow of the Arctic Basin and the Siberian Shelf Seas, 1996. Backbone Publishing Company, Fair Lawn, US.
39. RosHydromet, http://www.r-arcticnet.sr.unh.edu Last accessed: 30.07.2012
40. Rozman, P., Hölemann, J. A., Krumpen, T., Gerdes, R., Köberle, C., Lavergne, T., Adams, S., Girard-Ardhuin, F., 2011. Validating satellite derived and modelled Sea-ice drift in the Laptev Sea with in situ measurements from the winter of 2007/08. Polar ReSearch 30, 7218, doi:10.3402/polar.v30i0.7218Schättler et al. A Description of the Nonhydrostatic Regional COSMO-Model, Part VII: User's Guide [Book Section]. - 2008 : [s.n.].
41. Schröder, D., Heinemann, G., Willmes, S., 2011. The impact of a thermodynamic Sea-ice module in the COSMO numerical weather prediction model on simulations for the Laptev Sea, Siberian Arctic. Polar Res. 30, 6334, doi:10.3402/polar.v30i0.6334.
42. Simpson, J.H., Crawford, W.R., Rippeth, T.P., Campbell, A.R., Choak, J.V.S. , 1996. Vertical Structure of turbulent dissipation in shelf seas. Journal of Physical Oceanography 26(8), 1580-1590.
43. Sof'ina, E.V., 2008. The simulation of tidal ice drift and ice-related changes in tidal dynamics and energy in Siberian continental shelf. Dissertation, Russian State Hydrometeorological University (in Russian).
44. Steele, M., Ermold, W., 2004. Salinity trends on the Siberian shelves. Geophysical Research Letters 31, L24308.
45. Steppeler, J., Doms, G., Schättler, U., Bitzer, H.W., Cassmann, A., Damrath, U., Gregoric, G., 2003. Meso-gamma scale forecasts using the nonhydrostatic model LM.s.l. Meteorol. Atmos. Phys. 82, 75–96, doi:10.1007/s00703-001-0592-9.
46. Stroeve, J., Frei, A., McCreight, J., Ghatak, D., 2008. Arctic sea-ice variability revisited, Ann. Glaciol. 48, 71–81, doi:10.3189/172756408784700699.
47. Timokhov, L. A., 1994. Regional characteristics of the Laptev and the East Siberian seas: climate, topography, ice phases, thermohaline regime, circulation. Ber. Polarforsch. 114, L04501, doi:10.1029/2004GL021810.
48. Willmes, S., Adams, S., Schroeder, D., Heinemann, G, 2011. Spatio-temporal variability of polynya dynamics and ice production in the Laptev Sea between the winters of 1979/80 and 2007/08. Polar Research 30 (5971), doi:10.3402/polar.v30i0.5971.

49. Yang, D., Liu, B., Ye, B., 2005. Stream temperature changes over Lena River Basin in Siberia. Geophys. Res. Lett. 32, L05401, doi:10.1029/2004GL021568.
50. Yang, D., Kane, D. L., Hinzman, L., Zhang, X., Zhang, T., Ye, H., 2002. Siberian Lena River hydrologic regime and recent change. J. Geophys. Res. 107(D23), 4694, doi:10.1029/2002JD002542.
51. Zakharov, V. F., 1966. The role of flaw leads off the edge of fast ice in the hydrological and ice regime of the Laptev Sea. Oceanology 6, 815–821.